



Control and Protection Paradigms of the Future

Future Grid Thrust Area 2 White Paper

Power Systems Engineering Research Center

*Empowering Minds to Engineer
the Future Electric Energy System*



Thrust Area 2 White Paper

Control and Protection Paradigms of the Future

Project Team

C.L. DeMarco, C.A. Baone, B.C. Lesieutre, Y. Han
University of Wisconsin-Madison

A. Bose, P. Kansal
Washington State University

M. Kezunovic, B. Matic-Cuka
Texas A&M University

PSERC Publication 12-10

May 2012

For information about this white paper contact:

Christopher L. DeMarco, Professor
Department of Electrical and Computer Engineering
University of Wisconsin-Madison
2544 Engineering Hall
1415 Engineering Drive
Madison, Wisconsin 53706
Phone: 608-262-5546
Email: demarco@engr.wisc.edu

Power Systems Engineering Research Center

The Power Systems Engineering Research Center (PSERC) is a multi-university Center conducting research on challenges facing the electric power industry and educating the next generation of power engineers. More information about PSERC can be found at the Center's website: <http://www.pserc.org>.

For additional information, contact:

Power Systems Engineering Research Center
Arizona State University
527 Engineering Research Center
Tempe, Arizona 85287-5706
Phone: 480-965-1643
Fax: 480-965-0745

Notice Concerning Copyright Material

This copyrighted document may be distributed electronically or in print form as long as it is done (1) with the entire document including the cover, title page, contact page, acknowledgements, and executive summary in addition to the text, and (2) attribution is given to the Power Systems Engineering Research Center as the sponsor of the white paper.

© 2012 University of Wisconsin-Madison. All rights reserved.

Acknowledgements

The support for research on electric energy challenges for the future came from an initiative funded by Office of Electricity Delivery and Energy Reliability, U.S. Department of Energy under a project entitled “The Future Grid to Enable Sustainable Energy Systems: An Initiative of the Power Systems Engineering Research Center.” More information about the Future Grid Initiative is available at the PSERC website.

The authors also acknowledge valuable discussion and comments among their colleagues in the Power Systems Engineering Research Center, under whose auspices this work was done.

Executive Summary

This is a white paper that reports on both research progress and anticipated research challenges related to the future power grid in the United States. Its central theme is an examination of opportunities for improved grid control created by the growing penetration of advanced measurement, communication and embedded computation, with a particular emphasis on how these technologies can allow the power grid take maximum advantage of high penetration of renewable energy sources. The existing U.S. power grid has a strong foundation of practice in system regulation and protective relaying on which to build; however, it is the premise of this paper that new technologies in energy production and storage (e.g., renewables), expanded participation of responsive loads, and the new hardware for measurement, communication and computation will demand new architectures for grid control and protection.

The North American power grid has long reflected its underlying physics and organization in a hierarchy of control actions, from very fast actions that utilize purely local information, to more centralized, wider-area coordination that uses information across a large geographic footprint. The work here will continue advocate a mix of both hierarchical and distributed sensing and decision architectures, but with new features to reflect the capabilities of evolving technology. Most specifically, we anticipate the ability of distributed elements to employ more computational intelligence and better measurements to estimate the state of the network around them, even when these measurements remain predominantly local. Conversely, we anticipate greater availability of low latency, high bandwidth communication, that when designed with appropriate levels of security and robustness can allow wide-area sensing and decision-making to operate on a much faster time scale than in the past. Roughly speaking, we envision a future in which local, smaller-scale elements (e.g., smart loads) have can greater reach “upward,” taking greater account of system-wide objectives as they exercise their control and protection actions. At the other end of the hierarchy, we envision wide area decision-making and control with high speed and bandwidth, allowing central coordination to have further and faster reach “downward,” communicating system needs and status to distributed grid players more accurately and more frequently.

Table of Contents

1. Introduction.....	1
2. Research Topics	2
2.1 Overview.....	2
2.2 Inter-Relationships of the Research Areas.....	2
3. Requirements for Hierarchical Coordinated Control and Protection of the Smart Grid.....	4
3.1 Objectives and Methodology	4
3.2 Context and Significance of this Research	4
3.3 An Umbrella Architecture for Communication/Control/Protection	5
3.3.1. Introduction	5
3.3.2. Infrastructure Components	5
3.3.3. Smart Grid Applications.....	7
3.3.4. Smart Grid Communication	8
3.3.5. Simulation Results.....	11
3.3.6. Conclusions	22
4. Hierarchical Coordinated Control of Wind Energy Resources and Storage for Electromechanical Stability Enhancement	24
4.1 Objectives and Methodology	24
4.2 Context and Significance of this Research	24
4.3 A Hierarchical Multi-input/Multi-output Design Method	26
4.4 The System Model	29
4.4.1. Modeling Power Injection Variation Disturbances to be Regulated.....	29
4.4.2. The IEEE 14 Bus Test System	30
4.4.3. Modeling of the Actuators.....	30
4.4.4. Implementation of the Control Design.....	32
5. Hierarchical Coordinated Protection of the Smart Grid with High Penetration of Renewable Resources	41
5.1 Objectives and Methodology	41
5.2 Context and Significance of this Research	41

5.3	New Architectures for Coordinated, Hierarchical System Protection	42
5.3.1.	Predictive Protection	43
5.3.2.	Inherently Adaptive Protection	47
5.3.3.	Corrective Protection.....	50
5.3.4.	Study Case	54
5.3.5.	Future Work	57
6.	Conclusions.....	60
	References.....	61

List of Figures

Figure 1: Real Time Information Infrastructure for the Electric Power Grid.....	6
Figure 2: Communication Architecture	9
Figure 3: Snapshot of 14 Bus NS2 Simulation with 6 Traffic Types	11
Figure 4: Polish Power System Zones	18
Figure 5: Communication Topology to Connect Control Centers for Polish System	21
Figure 6: Conceptual Block Diagram Illustrating Exosystem Role.....	31
Figure 7: Time Plot of Load Disturbance–Fast Time Scale Periodic Switching Selected as a Representative “Worst Case” Disturbance Against Which Controller Must Regulate.....	34
Figure 8: Actuator Signals Nominal Case	34
Figure 9: Weighted Output–Nominal Case.....	35
Figure 10: Battery Output–Open Loop Case	35
Figure 11: Actuator Signals–Open Loop Case	36
Figure 12: Weighted Output–Open Loop Case	36
Figure 13: Actuator Signals–Saturation Case	37
Figure 14: Frequency Deviation Performance–Saturation Case.....	37
Figure 15: Actuator Signals–Case of Control Design Accounting Saturation	38
Figure 16: Frequency Deviation Performance–Case of Control Design Accounting Saturation	38
Figure 17: Battery Output Signals–Saturation Case	39
Figure 18: Battery Output Signals–Control Designed to Remain within Limits.....	39
Figure 19: Actuator Signals–Observer Based Scheme	40
Figure 20: Fuzzy ART Neural Network Training Process for Fault Diagnosis Algorithm.....	48
Figure 21: Formation of Patterns During Training and Testing	48
Figure 22: Architecture of Neural Network Training	49
Figure 23: Synchronized Sampling Based Fault Location	50
Figure 24: A Faulted Transmission Line	51
Figure 25: Steps for Long Line Fault Location Algorithm.....	52

Figure 26: No Fault Condition.....	53
Figure 27: The Hierarchical System Protection Architecture.....	54
Figure 28: IEEE 39-Bus System.....	55
Figure 29: Event Sequence	56
Figure 30: Trajectory of Impedance	56
Figure 31: Overcurrent Under-Reach [69].....	57
Figure 32: Thevenin Equivalent of the System with and without DG [69].....	58
Figure 33: Overcurrent Sympathetic Trip [69]	58

List of Tables

Table 1: Survey of Smart Grid Applications Based on Latency & Data Requirements....	9
Table 2: Protocol Layers for Communication in One Control Area.....	10
Table 3: WECC Statistics Ffter Node Reduction	14
Table 4: Packet Size of Traffic Type-1	14
Table 5: Link Bandwidth Usage	15
Table 6: Maximum Delays for Different Traffic Types	15
Table 7: Queuing Delays	16
Table 8: Number of Hops	16
Table 9: Assumed Bandwidth for Simulations	17
Table 10: Delays in WECC System with Varying Bandwidth	17
Table 11: Actual Link Bandwidth Requirement for WECC.....	17
Table 12: Overall Statistics of the Polish System.....	19
Table 13: Zonal Statistics of the Polish System.....	19
Table 14: Packet Size of Traffic Type-1	19
Table 15: Average G2G Link Bandwidth Usage in Mbps.....	20
Table 16: Maximum Delays in Traffic for Each Zone	20
Table 17: Number of Hops	20
Table 18: File Size of Raw Measurements and Breaker Status	22
Table 19: Delay for Inter Control Center Communications	22
Table 20: Delay in Exchanging Complete Information Across Polish System.....	22
Table 21: Scenarios and Reference Actions for the Nodes of Event Tree.....	53

1. Introduction

With widespread discussion of the “smart grid” in both the professional and the popular press, it has become well accepted that new information technologies will enable the North American electric power system to enhance its control and protection schemes to increase its reliability and the efficiency. Broadly speaking, such improvements represent a significant piece of the promise of the smart grid. Moreover, the trend towards higher penetration of non-traditional, power-electronically coupled renewable generation resources will be very dependent on our ability to develop these schemes. Customized solutions for grid operation challenges in targeted locations are a current focus of research and development, and some solutions, like system integrity protection schemes (SIPS), are already in use.

However, these one-of-a-kind special control and protection are very expensive. A streamlined process for the design, installation, operation and maintenance of such control/protection schemes and the conceptual framework for these problems needs to be developed. New technologies are making it possible to move from protection and primary control that relies local information and meets (predominantly) local objectives, and instead move towards distributed control and protection devices that use more wide area information and reflect more system-wide objectives. The new framework has to be **hierarchical** so that both subsystems and the whole system can be covered and at the same time **coordinated** both across the power system (geographically) as well as across the voltage levels.

The work of the research thrust reported in this white paper seeks to develop the principle of **hierarchical coordinated control and protection** of the smart power grid. This work is pursued with a major companion goal of incorporating more renewable generation resources while increasing reliability and efficiency. The task under this research thrust have been structured to comprehensively look at this subject from the development of the theory to the engineering design to the testing of hierarchical coordinated control and protection.

2. Research Topics

2.1 Overview

The research thrust area that underlies this white paper has three topics that will be examined and analyzed:

1. The first topic relates to the requirements for the communication and computation architecture for hierarchical coordinated control and protection. Unlike many other operational functions, control and protection have stringent requirements for the latency of measurement and control signals.
2. The second topic is the hierarchical coordinated control of for stable electromechanical response accounting for the impact of high penetration power electronically-coupled renewable generation and storage. The coordination for off-line, on-line and real-time becomes more crucial with such system wide controls, as do designs that make use of more detailed dynamic estimate of system states.
3. The third topic focuses on hierarchical coordinated protection. A different approach to protection design is proposed where local protection is coordinated with logic at local and regional levels, and higher. At these fast speeds, control and protection are difficult to separate as concepts (protection can be considered digital control). However, the long tradition of protection engineering and the increasing use of SIPS provide methodologies that can be used in developing the new fast controls.

2.2 Inter-Relationships of the Research Areas

With the exception of a small number of customized “special protection schemes,” the arenas of power system protection and power system dynamic control have historically been “silo-ed,” with each design process proceeding largely independent of the other. Traditionally, such a division was judged reasonable, as each arena focus on largely distinct objectives. Protection, as its title suggests, focus primarily on the “equipment-centric” problem of protecting individual pieces of hardware from damage due to emergency overload conditions. Dynamic control focused more on the “system-wide” objectives of regulating frequency, voltages, power injections and flows to a desirable operating point, all while maintaining the stable transient response of the system in the event of large disturbances. It has long been recognized that there can be situations in which local objectives (and pursued by protection) and system wide objectives (as pursued by dynamic control) may come into conflict, and yield less than optimal performance under certain disturbance scenarios. It is the premise of this work that as we seek to incorporate a much more diverse set of renewable energy producers and smart grid contributors, the traditional “siloining” of protection and dynamic control will become increasingly unacceptable; simply put, it will become important to co-design and jointly optimize the impact of these two. Viewed abstractly, protection is a class of discontinuous switching actions that either disconnect individual pieces of equipment, or in some scenarios, change the topol-

ogy of the network. These can be interpreted as a class of discrete “control actions;” albeit these are actions with typically large impact and sometimes high cost. However, with appropriately formulated objective functions to represent the cost and impact of activating protective relaying, conceptually they may be unified with continuously acting control actions in an optimal control analysis. However, while conceptual simple, the analytic and practical challenges in such an integration are huge, and require far more than direct application of textbook optimization and optimal control algorithms. Rather, the authors see critical need in careful blending of domain specific expertise in power systems operations with application of more advanced optimization-based control design techniques. These needs become even more apparent as the third leg of advanced smart grid technology is incorporated, that of wide area measurement and communication. While the rapid growth in advanced relays, substation automation, and Phasor Measurement Unit deployment all bring much higher quality sensing, there remain issues in low-latency, high bandwidth, and highly secure communication of measurements that present significant challenges. The authors also believe that these measurement and communication characteristics must be reflected in the more unified control and protection architectures of the future.

3. Requirements for Hierarchical Coordinated Control and Protection of the Smart Grid

3.1 Objectives and Methodology

The main objective in this aspect of the work is to define an overall concept for hierarchical coordinated control and protection of the smart grid. Although individual control or protection schemes have been proposed and developed to aid in solving particular problems, there is yet no clear picture of an overall unifying architecture of controls and protection that can aid the smart grid. The fact that controls will encompass wide areas as well as several voltage levels is now accepted as realizable because of the fast communications and computation available, but how all of these controls will be coordinated has not been thought out. This task assumes that a hierarchical and distributed structure will be used and the main objective is to determine the requirements for this structure.

The methodology is the time simulation of communication and computation infrastructure that is compatible with the time simulation of the power grid. That is, the time simulation of power grid behavior will include the simulated behavior of the communication and computation (something that is missing in present day power grid simulations). Although simulation of communication networks is not new, how to model and simulate communication networks and computation delays together with the power grid simulation has to be understood. By simulating the IT infrastructure together with the power grid for different hierarchical coordinated control and protection schemes, the requirements of the IT infrastructure can be determined. The scope and methodology is developed further in the four subtasks below.

3.2 Context and Significance of this Research

In this thrust the framework for the wide area control and protection will be developed. Such a framework can be used to design new adaptive wide area control/protection instead of designing each scheme as a separate and unique one. Such a framework will be hierarchical and coordinated, which can support schemes that can encompass system wide control/protection to local control/protection and any combination thereof. This task defines the IT portion of the framework – the communication and computation infrastructure. If the same IT framework is used as the basis of all control/protection schemes then the design of the scheme ends up being an engineering design process to meet the most stringent requirements rather than a complete (and separate) design of a unique (and expensive) custom solution. This is the basic part of the framework and the next three tasks develop the approach for stability control, voltage control and protection schemes as the three major control and protection categories. The final task sets up the requirements for testing any such hierarchical coordinated control/protection schemes. The whole thrust is devoted to the development of the systemic approach which can be used to conceptualize, design, test and install hierarchical coordinated control and protection. This task addresses the communication and computation portion of the framework.

3.3 An Umbrella Architecture for Communication/Control/Protection

3.3.1. Introduction

Most of the new applications being conceived today as a result of much greater communication and computation capabilities, as well as the supporting information software, are dependent on transitioning to a new type of architecture envisioned in Figure 1. This architecture assumes a significant infusion of new measurements (synchrophasors), communications and control devices (FACTS). It is not going to happen overnight, but will have to be phased in over many years both because of the costs involved as well as the fact that the system has to be fully operational during the transition. Thus the transition has to be planned carefully, i.e. while certain parts of the transmission grid is upgraded, these new information handling and applications can be tested and implemented on these parts, and the rest of the grid can be cut over as it is upgraded.

3.3.2. Infrastructure Components

Phasor Measurements

So far phasor measurement units have been installed in an ad hoc way with no particular applications in mind. A systematic goal may be to make observable regions with phasor measurements. First only a few substations could be made observable, then their neighboring substations can be added, and so on. Moreover, it would be reasonable to start with the highest voltage substations, because they will be the easiest to retrofit as they are usually the newest and because they will have the most impact on any application. The feasibility of installing so many phasor measurements—tens of thousands rather than tens—is fully dependent on the fact that all new measuring, recording and control equipment in the substation are microprocessor based and capable of synchronizing through a GPS signal.

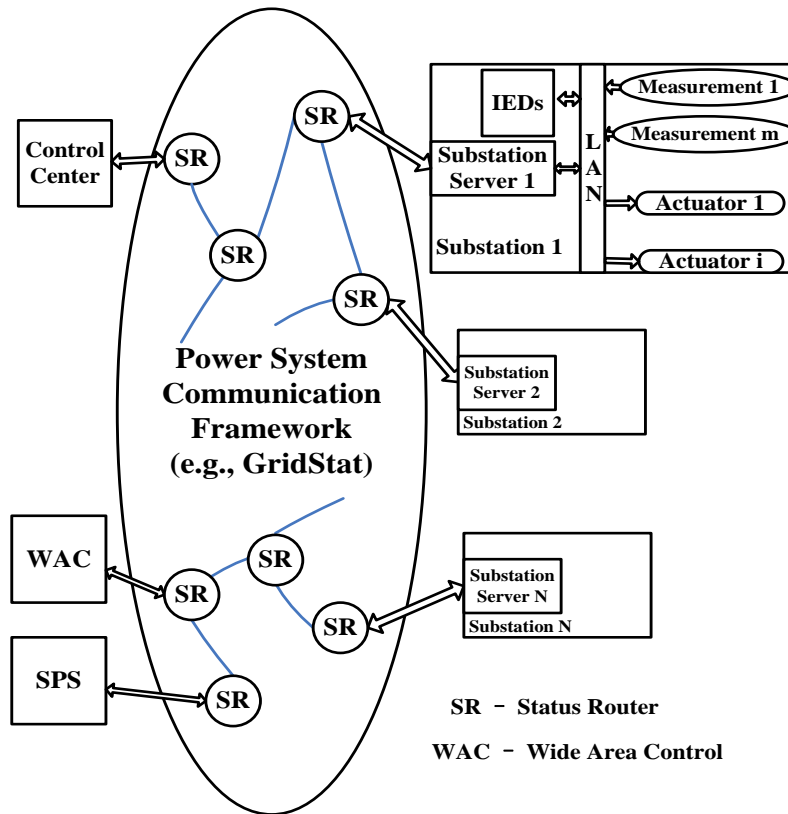


Figure 1: Real Time Information Infrastructure for the Electric Power Grid

Communications

The development of the communication system can follow the synchrophasor implementation at substations. As more phasor measurements are installed at a substation, a digital LAN within the substation will be needed to handle its collection and handling as well as a gateway server as shown conceptually in Figure 1. A managed meshed network is needed to connect all these updated substations and other application servers. This multi-level communication system will require significant software (middleware) development.

Controls

The most useful applications for smart operation of the transmission system are fast wide-area controls. To implement these we will need fast controllers, i.e. FACTS devices. Except for FACTS, we are limited to the opening and closing of circuit breakers for our only fast controls and such digital control is quite limited in scope. Because of their expense, the number and type of FACTS controllers will have to be carefully selected (at least until their prices come down) but this would be easier to do once the measurements and communication parameters are known.

Databases

With thousands of phasor measurements updating 30, 60 or 120 times per second, centralizing the real time database is not feasible. Thus the database has to be a distributed one, also depending on the communication system to move data where it is needed. This means that the applications will also be distributed, which in turn, implies that our static

database is also distributed. The design and development of this database will be a significant undertaking (somewhat similar in scope as the design of the communications system).

Simulation and Design of Applications

Although it is clear that such an infrastructure can support better automatic controls and better operator tools, the actual tools and controls are yet to be developed. The development of these applications will require significant R&D. In fact the tools required for this development are woefully inadequate and will have to be developed first.

Take for example, the simulation tools that are used for planning today: power flow and transient analysis. The models used in these simulations are simple; a bus-branch model that does not have any description of the substation details and hence no way to model the fine-grained control systems within a substation like protection. Thus the representation of actual measurements and breaker openings by even local protection is not feasible. In addition, the models are single phase balanced systems whereas actual protection and control schemes operate more for unbalanced faulted systems. To design a fast wide area controller that uses PMU inputs we will need to represent it in a time simulation of the grid where the time granularity of the simulation must match the time granularity of the controller. Such simulation tools with the time granularity and the models are not available at this time.

3.3.3. Smart Grid Applications

Measurements

The data which we need in real time for successful analysis, operation and control of the grid is its topology and state. The topology defines the interconnection of the grid and is almost constant over time [13]. On the other hand, the state (voltage and angle at all buses) of the power system changes dynamically over time due to changes in loads, generation and switching operations. Without PMUs, state of the grid is derived from voltage magnitude (V), real power (P) and reactive power (Q) measurements using a computer program called State Estimator (SE). Most of the power grid applications based on this set-up are bottlenecked by the latency and accuracy of the estimated state of the system as calculated by state estimator. As these measurements are collected by Supervisory Control and Data Acquisition (SCADA) system by polling over 2-4 seconds, the measurements do not represent a snapshot of the actual system state at one particular time. This set-up seems to work fine for an unstressed grid working in almost steady state conditions. The present operation of the grid is often very close to its security margins and the system venture into the emergency state more frequently than before. State-estimator cannot capture the changing state of the system and sometimes fails to converge. With PMUs all over the system, the state of the grid (voltage phasors) can be directly measured and moreover can be measured many times per second with time-stamps giving insight into the dynamics of the system.

Current Status

A number of smart grid applications have already been developed and some are in the process of development [11]. To understand their communication needs, a brief survey of some of the most important applications in terms of their data requirement and latency is

presented in Section II.C and Table 1. A communication network designed to handle these basic applications would be able to handle other applications as well.

Classification

1. *State Estimation*: Even though voltage phasors across the grid can be directly measured with PMUs everywhere, state estimation is an essential tool to eliminate effect of bad measurements on the final calculation of the state. Most of the Energy Management System (EMS) applications are fed from state estimated data and are benefited by faster, accurate and synchronized measurements. Also with PMUs, two level state estimators [14] can be designed to run locally within the substation to feed applications like transient stability.
2. *Transient Stability*: Transient stability is a concept related to the speed and internal angles of the generators. A typical system can get transiently unstable in approximately 10 cycles. The way to prevent this is to island the system in coherent groups or shed load/generation using Special Protection Schemes (SPS). The wide-area control to do so is still not in place because of latency requirements and it would be a big challenge to design such a control system even in the future.
3. *Small Signal Stability*: To solve small signal stability problem, we need signals only at selected key locations where modes are more visible. For any of these modes, if damping happens to change then it changes slowly over time. Moreover, if the damping is negative, even in that case, oscillations take time to build. So small signal instability occurs over a period of time and by observing the mode damping near real time this can be prevented by resetting the power flows across the lines or by setting Power System Stabilizer (PSS) online.
4. *Voltage Stability*: Voltage instability spreads over time starting from reactive power (VAR) deficient area and can ultimately cascade and lead to a blackout. The problem can be solved if the voltage in an area can be measured and corrected by balancing VAR in the particular area or by islanding the area.
5. *Post-Mortem Analysis*: This will be a key application to correct power system models and to update engineering settings for the system. The engineering settings are bound to change as the system changes. This application does not need to run real time and has no latency requirements. This application will require PMU data as well as data from other IEDs (Intelligent Electronic Devices) like DFRs (Digital Fault Recorders).

3.3.4. Smart Grid Communication

Infrastructure

We assume smart grid of the future will have PMU data available across the grid. To meet the latency requirements and to handle the huge amounts of data, a real time information infrastructure was proposed [13]. Because of the huge amount of data generated at each substation, not all the data can be sent to one central location. Therefore, there is a need for the application servers to be distributed as shown in Figure 2. Separating out application servers will also help to tag packets for latency purpose. The middleware system to handle this distributed data base and to provide the latency and other Quality of Ser-

vice (QoS) is one of the major goals of the NASPI [11-12] and some research initiatives like Gridstat [15-16].

Table 1: Survey of Smart Grid Applications Based on Latency & Data Requirements

Main Application	Applications based on it	Origin of Data/Place where we need the data	Data	Latency requirement	Number of PMUs we may need to optimally run the application	Data time window
<i>State Estimation</i>	Contingency analysis, Power flow, AGC, AVC, Energy markets, Dynamic/ Voltage security assessment	All substations/ Control center	P,Q, V, theta, I	1 second	Number of buses in the system	Instant
<i>Transient Stability</i>	Load trip, Generation trip, Islanding	Generating substations/ Application servers	Generator internal angle, df/dt, f	100 milliseconds	Number of generation buses (1/20 buses)	10-50 cycles
<i>Small Signal Stability</i>	Modes, Modes shape, Damping, Online update of PSS, Decreasing tie-line flows	Some key locations/ Application server	V phasor	1 second	1/10 buses	Minutes
<i>Voltage Stability</i>	Capacitor switching, Load shedding, Islanding	Some key location/ Application server	V phasor	1-5 seconds	1/10 buses	Minutes
<i>Postmortem analysis</i>	Model validation, Engineering settings for future	All PMU and DFR data/Historian. This data base can be distributed to avoid network congestion	All measurements	NA	Number of buses in the system	Instant and Event files from DFRs

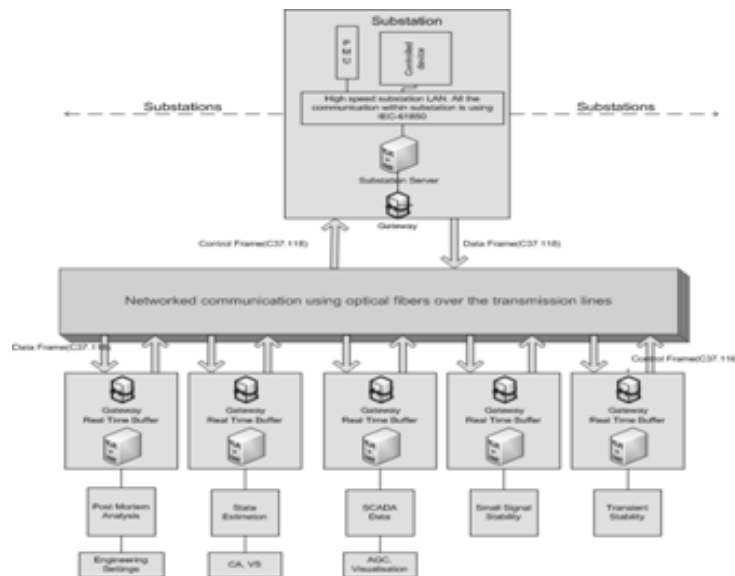


Figure 2: Communication Architecture

PMU Data Format (C37.118)

The standard mostly used in practice for PMU data format is C37.118 [17]. Among the four frames that are defined in C37.118, Data Frame is the one that is sent out from substation during normal system operation. Hence, it is important to know the data formats to exactly evaluate how much data is being generated in bytes at each substation. Also, one data frame can carry data from multiple PMUs.

Latency

We define data latency as the time between when the state occurred and when it was acted upon by an application. Each application has its own latency requirements depending upon the kind of system response it is dealing with. Among the other delays [18], communication delay also adds to the latency and need to be minimized. The communication delays on the network are comprised of transmission delays, propagation delays, processing delays, and queuing delays [1]. Each of these delays must be looked into to understand the complete behavior of the communication network for a given network.

Communication within One Control Area

The data from various PMUs from a substation is sent out in C37.118 format Data frame. This data is then received at the location of the application in its respective Phasor Data Concentrator (PDC) usually using proprietary software; the only open source software called Open-PDC is used in this paper.

We know that PMUs are constantly sending out the data frame on the network. For many of the smart grid applications latency is an important consideration in designing a communication infrastructure. Keeping this in mind, User Datagram Protocol (UDP) becomes a preferred protocol at the transportation level over Transportation Control Protocol (TCP). At the application layer, Constant Bit Rate (CBR) is a good choice to carry the continuously generated data frames of PMU. Maximum Transmission Unit (MTU) size of the link layer will play an important role as OpenPDC is designed to receive a complete C37.118 packet and not a broken one. As shown in the simulations, packet size can be around 1500 bytes, i.e. Ethernet communication having MTU size as 1500 bytes is the obvious choice. Given the latency and bandwidth requirements, optical fibers and Broadband over Power Line (BPL) are the promising solutions. For uniformity we assume that optical fiber is present throughout the network. Hence the protocol stack will look like as shown in Table 2.

Table 2: Protocol Layers for Communication in One Control Area

Layer	Protocol
<i>Application</i>	CBR
<i>Transportation</i>	UDP
<i>Network</i>	IP
<i>Data</i>	Ethernet
<i>Link</i>	Ethernet (Optical fiber)

3.3.5. Simulation Results

Simulation Setup

Here we present the simulation results for Western Electricity Coordinating Council (WECC) 225 bus system and Poland 2383 bus system [19]. We simulated one of the possible communication scenarios using an event based, open source communication network simulator called NS2 version 2.34 [20, 21]. We further wrote Matlab, Python, Tcl and Awk scripts to do the analysis. We identified the following 7 basic traffics in the network as shown in the simulation snapshot for IEEE 14 bus system in Figure 3:

1. All the Substation (S/S) to Control Center (CC)
2. Control Center to Control Substation (Generating stations and substation having control units like transformers and reactors)
3. Special Protection Scheme (SPS) substation to SPS
4. SPS to SPS substation
5. Generating substation to Generating substation
6. SPSs to Control Center
7. Control Center to Control Center

Here, SPS is used generically to represent any wide-area closed-loop control and/or protection. An SPS may not be located at the control center or at any substation and it needs data only from a few locations and issues commands back to few substations only. SPS can be especially useful for transient stability applications where latency is of significant importance.

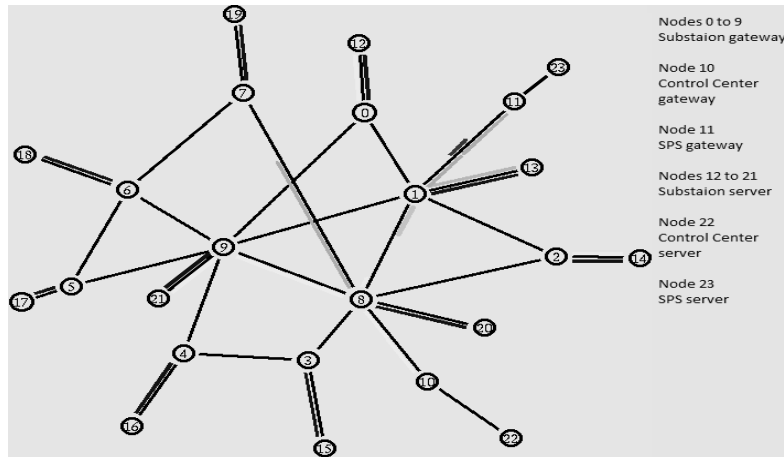


Figure 3: Snapshot of 14 Bus NS2 Simulation with 6 Traffic Types

The key assumptions that we have to make in the simulation are discussed in the previous sections. Similar network simulations [22] have been carried out before and some of the assumptions in this paper are similar to [18, 22-24]. The main difference in this work is that the assumptions are developed by starting from the power network, substation configurations and anticipated on-line applications (Section IV.B) to determine the data

transfer needs. Different scenarios can be studied using different protocols, routing algorithms, data formats, sampling rates, and communication infrastructure. Also, accuracy of the results would depend on the modeling details and some of it may require changing the NS2 source code. This paper focuses on presenting a methodology to simulate a possible communication scenario using power system topology information with design parameters based on smart grid application requirements.

Assumptions for Power Systems Data

The information that is required to calculate the amount of data for an actual power system is substation configuration and connected equipment (generators, reactors, and transformers). Location of the application servers (control center and SPS) and location of controls along with their individual data needs then define the amount of data that need to be communicated. For a real power system this information is easily available.

The connection between substations is from the given power system network data and the communication network overlays that. In case of multiple transmission lines between two substations, only one communication link is considered to connect them. Control center (CC) node is connected to the substation node having maximum number of communication links. This will allow distribution of traffic to the CC node through multiple paths. Similarly SPSs are connected to the available substation nodes having maximum connectivity. This completes a communication network graph of network gateways for a given power system.

Each gateway is connected to a server. Power system applications and PDCs are running in these servers. As an integrity check and to run communication simulation, we wrote a computer program to verify the connectivity of the network graph obtained after this step.

The second step is to estimate packet sizes in each of these substations, control centers and SPSs. We calculate packet size for data traffic between substation and control center (type-1 traffic) as follows:

1. The configuration for each substation is usually known (in our examples we assume a breaker and half scheme for all substations). The 3 phase quantities for each section and CB status are measured and communicated.
2. Channels for each PMU are known (assumed to have 9 analog channels and 9 digital channels in examples below).
3. Given the number of PMUs and number of phasors in a substation, the size of C37.118 data frame is calculated.

Types-2 through-6 traffic have packet sizes smaller than the type-1 traffic because only selected data for control purposes constitutes these types.

For the two example power networks, we had the power network data but not the substation details. The identification of substation configurations, control substations, control centers and SPSs is a first step to determine the data traffic for our simulation studies. We wrote a computer program to do this step. We combine buses that are connected through transformers into one communication node per substation. We then calculated the number of feeders in each of these substations. On top of the substation, we added one control

center per zone where we treated each zone as one control area. We then added SPSs assuming that a group of approximately 10 substations will be connected to one SPS.

Assumptions for Communication Simulation

After obtaining the network graph and data requirements, the following assumptions are made for communications:

1. As discussed earlier, we used CBR over UDP to simulate the traffic with MTU size as 1500 bytes.
2. As a base case, we assumed duplex links of sufficiently high bandwidth between substations as OC-3 i.e. 155 Mbps and the receiving link for the CC/SPS as OC-12 i.e. 622 Mbps.
3. To observe larger queuing delays and to avoid packet drops, based on few simulation runs, we assumed the queue size as 5000 packets.
4. To simulate large network such that every packet reaches its destination node without being dropped, based on few simulations run, we set the Time-To-Live (TTL) value to 64 hops.
5. Number of CC and SPSs are chosen based on the size of the network.
6. Data set out from the substation/SPS/Control center server is in C37.118 format (fixed 16-bit).
7. The routing used by NS2 is the shortest route (number of hops) and is kept default as static.
8. We assumed that the system is under normal operation and only Data frames are being communicated.
9. The sampling rate is assumed to be 60 samples/second for all the traffic sources.
10. The processing delays in gateways (10-100 microseconds [25]) are assumed to be zero. Here gateways are considered as forwarding nodes only to simulate communications. Data aggregation/ processing occur at end nodes/PDC only and we consider this delay as computation delay and not communication delay. The computation delays can be added at each end node for specific application without making it a part of the communication simulation.
11. We assumed that the communication is uniform i.e. no spikes in data.
12. To calculate propagation delay, we converted the network reactance into miles [26].
13. Propagation delay between server and gateway is assumed to be 1 microsecond.

NS2 simulation is run after following the steps/assumptions above. NS2 generates a trace file with all the events (packet drop, packet receive, etc.) for each packet generated in the system. These files are analyzed using various computer programs [27] for results on latency and bandwidth presented below.

WECC Results

WECC 225 Bus Power System

The WECC 225 bus is a reduced model of the WECC transmission network though representing almost same geographical area. Power system statistics after following the methodology discussed earlier are presented in Table 3. Note that we have only one control center and hence six traffic types for WECC.

Table 3: WECC Statistics after Node Reduction

S.No.	Parameter	Value
1	<i>Buses</i>	225
2	<i>Substations</i>	161
3	<i>Control Center</i>	1
4	<i>SPS</i>	16
5	<i>Generating S/S</i>	31
6	<i>Control S/S</i>	58
7	<i>SPS S/S</i>	160

Packet Size

As shown in Table 4 the maximum packet size for type-1 traffic in a substation can be as much as 1540 bytes. Also, packet sizes for a given power system would be same for all communication topologies. We assumed type-1 to type-6 traffic packet size to be 250 bytes for the simulation purposes which is lower than the median of type-1 packet size.

Table 4: Packet Size of Traffic Type-1

Maximum (Bytes)	Minimum (Bytes)	Average (Bytes)	Median (Bytes)
540	148	401	280

Average Link Usage for Different Communication Topologies

As shown in Table 5, we did simulation for four different cases. In the first simulation we used Kruskal's algorithm [28] to get minimum spanning tree (S.T.) for the communication network. This gives us the minimum number of links required for networked communication of a given power system. In next three simulations we used the complete graph as obtained after node reduction program with variation in number of control center links, for example, 3 CC link means connecting CC gateway to the three substation gateways (with maximum connectivity) in the network. Clearly, connecting control center with some substations geographically distant is really important as it makes the routing really efficient by avoiding bottlenecks and providing alternate shortest path to the traffic. Also, we must not use spanning tree configuration from reliability perspective.

For full topology case, by adding just 4 more CC links we can save 40% on link usage and delays reduces to ¼ for 5CC link configuration compared to 1CC link configuration. Hence, this helps in decreasing delays by adding just few links. Also, notice that average bandwidth usage decreases because now packet takes shorter route and traverses lesser link to reach its destination.

Table 5: Link Bandwidth Usage

Topology	Max. of used links (Mbps)	Min. of used links (Mbps)	Average of used links (Mbps)	Median of used links (Mbps)	% of un-used Gw2Gw links
<i>Min S.T.</i>	58.75	0.10	5.46	0.39	28.6%
<i>1CC links</i>	45.60	0.08	3.34	0.62	11.4%
<i>3CC links</i>	46.80	0.10	2.97	0.51	11.7%
<i>5CC links</i>	44.09	0.08	2.03	0.38	10.8%

Maximum Delays in Traffic for Different Communication Topologies

As shown in Table 6, we have figured out the maximum delays for the six identified traffic types. With the large bandwidth of fiber optics and meshed communication, it can be noted that maximum delays for all the traffic types are well within the latency requirements for most applications.

Table 6: Maximum Delays for Different Traffic Types

Network Topology	Type1 (ms)	Type2 (ms)	Type3 (ms)	Type4 (ms)	Type5 (ms)	Type6 (ms)
<i>Min S.T.</i>	49.9	40.3	45.1	46.3	44.0	40.3
<i>1CC links</i>	26.2	27.6	26.6	27.1	29.4	23.9
<i>3CC links</i>	19.2	19.1	25.2	25.5	29.3	16.4
<i>5CC links</i>	11.7	5.2	13.8	12.9	15.6	4.5

Queuing Delays

As shown in Table 7, we have calculated the queuing delays for each system. Notice that with the huge bandwidth available queuing delays are almost negligible. Queuing delay can increase really fast if the network get congested or if the bandwidths on incoming link and outgoing link are disproportionate.

Table 7: Queuing Delays

Topology	Maximum (μ s)	Minimum (μ s)	Average (μ s)	Links with queue delay as zero (%)
<i>Min S.T.</i>	586	0	17.7	53.1%
<i>1CC links</i>	441	0	13.7	60.1%
<i>3CC links</i>	259	0	12.0	60.2%
<i>5CC links</i>	354	0	12.6	60.8%

Number of Hops

As shown in Table 8, we have calculated the number of hops that a packet has to traverse assuming shortest hop routing algorithm. This data will help us understand how much an issue can processing delays at gateways can be if they happen to increase due to more intense routing mechanisms or other reasons like security.

Table 8: Number of Hops

Topology	Max	Min	Average	Median
<i>Min S.T.</i>	43	2	19	18
<i>1CC links</i>	28	2	12.2	12
<i>3CC links</i>	26	2	10.6	10
<i>5CC links</i>	15	2	7.0	7

Simulations with Varying Bandwidth

In above sections we calculated various network parameters using the base bandwidth mentioned in assumptions. In this section we assumed 3CC link configuration and used the estimated bandwidth above as the actual required bandwidth. Table X shows the result on delays when we varied the bandwidth on the gateway (Gw) to gateway links (G2G) as the multiple of actual bandwidth. Further for the first three cases of results in Table 10, we assumed same bandwidth on gateway to server (G2S) links as pointed in Table 9. Notice that when we scale the bandwidth, we should scale it on the complete network i.e. both on G2G and G2S links or else queuing delay increases. Also as shown in Table 10 by using twice the actual bandwidth we can get delays similar to base case. Recalculated bandwidth consumption for each case is shown in Table 11.

Table 9: Assumed Bandwidth for Simulations

Bandwidth	Base Case (D3-D6) (Mbps)	Actual Usage (Mbps)
<i>Btw CC server and CC Gw</i>	Duplex 622	50Mbps (Gw to Server) / 10Mbps(Server to Gw)
<i>Btw Sps server and Sps Gw</i>	Duplex 622	Simplex 2Mbps
<i>Btw S/S server and S/S Gw</i>	Duplex 155	Simplex 5Mbps
<i>Btw CC Gw and S/S Gw</i>	Duplex 622	Simplex Integer(actual)+1
<i>Btw Sps Gw and S/S Gw</i>	Duplex 622	Simplex Integer(actual)+1
<i>Btw S/S Gw and S/S Gw</i>	Duplex 155	Simplex Integer(actual)+1

Table 10: Delays in WECC System with Varying Bandwidth

Bandwidth of G2G links	Max. Delay (ms)	Avg. of Max Delay of each traffic type (ms)	Max. Queuing Delay(μs)	Avg. Queuing Delay(μs)
<i>Actual BW/2</i>	167.0	91.2	43736	3413
<i>Actual BW</i>	55.3	39.3	8018	694
<i>Actual BW*2</i>	40.8	31.3	8018	595
<i>Actual BW*2</i>	38.1	28.3	4009	342
<i>Actual BW*5</i>	32.1	24.0	1603	131
<i>622Mbps and 155Mbps</i>	29.3	22.4	259	12

Table 11: Actual Link Bandwidth Requirement for WECC

Communication infrastructure	Max. G2G Bandwidth (Mbps)	Average G2G Bandwidth (Mbps)	Median G2G Bandwidth (Mbps)
<i>Actual BW/2</i>	24	2.59	1
<i>Actual BW</i>	47	4.48	2
<i>Actual BW*2</i>	94	8.28	3
<i>Actual BW*2</i>	94	8.28	3
<i>Actual BW*5</i>	235	19.88	6
<i>622Mbps and 155Mbps</i>	622	194.56	155

Poland 2383 Bus System Results

Polish Power System

Polish power system discussed here is a high voltage power system of Poland above 110kV which is divided into 6 zones. Zone 1-5 is shown in Figure 4 [29]. Zone-6 represents all the tie lines connected to the neighboring countries. For simulation purposes we included each of the Zone-6 bus into the respective Zone 1-5 to which it is actually connected. Each zone will have its own Control center and the only interaction between zones is between their respective Control centers. The inter control center communication would have separate direct connection using optical fibers over transmission line. The number of substations being more than 225 in each zone, we used 5CC and 7CC link communication infrastructure to simulate traffic in each zone.

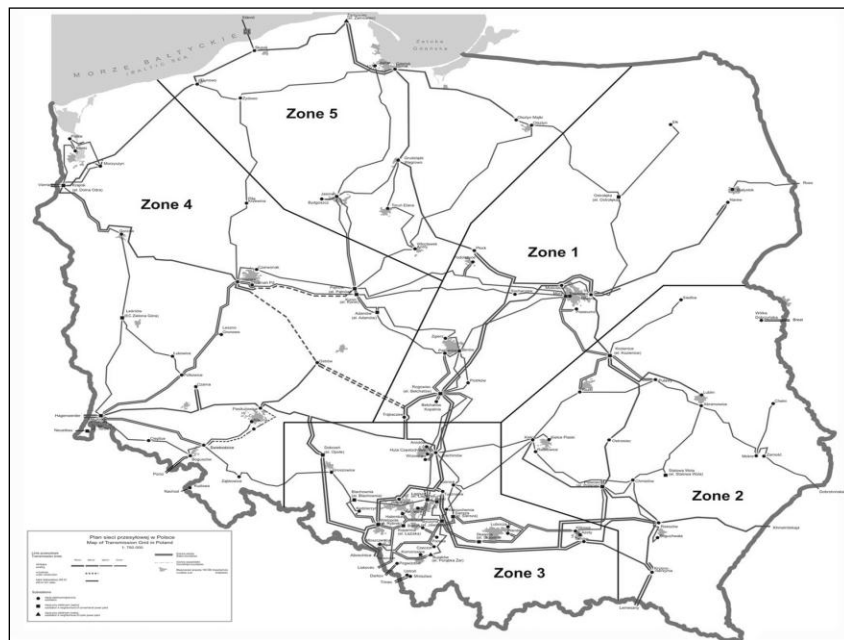


Figure 4: Polish Power System Zones

Network statistics following the above methodology are presented here in Table 12 and Table 13.

Table 12: Overall Statistics of the Polish System

S.No.	Parameter	Value
1	Buses	2383
2	Substations	2216
3	Control Center	6
4	SPS	219
5	Generating S/S	305
6	Control S/S	386
7	SPS SS	2190

Table 13: Zonal Statistics of the Polish System

Parameter	Zone1	Zone2	Zone3	Zone4	Zone5
Substations	343	259	831	515	268
Control Center	1	1	1	1	1
SPS	34	25	83	51	26
Generating S/S	42	36	88	92	47
Control S/S	56	51	104	112	63
SPS SS	340	250	830	510	260
CC links	5	5	7	7	5

Packet Size for Different Zones

After node reduction, we calculate packet size for data traffic for each zone as shown in Table 14.

Table 14: Packet Size of Traffic Type-1

Zone	Maximum (Bytes)	Minimum (Bytes)	Average (Bytes)	Median (Bytes)
1	1438	148	290.7	262
2	1204	160	303.1	262
3	1540	148	265.6	262
4	1426	148	281.2	262
5	1078	148	293.8	262

Average Link Usage for different Zones using 5CC/7CC Link Communication Topologies

The bandwidth usage is estimated only on the G2G links and is shown in Table 15.

Table 15: Average G2G Link Bandwidth Usage in Mbps

Max. of used links (Mbps)	Min. of used links (Mbps)	Average of used links (Mbps)	Median of used links (Mbps)	% of unused Gw2Gw links
126.77	0.09	4.68	0.94	2.96

Maximum Delays in Traffic for Different Zones

From our understanding of the WECC system we used twice the actual bandwidth usage as our new bandwidth and estimated the delays for the Polish system as shown in Table 16. This is well within the latency requirements for most applications.

Table 16: Maximum Delays in Traffic for Each Zone

Zone	Type-1 (ms)	Type-2 (ms)	Type-3 (ms)	Type-4 (ms)	Type-5 (ms)	Type-6 (ms)
1	12.4	11.5	22.2	28.7	23.6	11.9
2	12.7	10.8	19.7	24.6	25.3	10.2
3	14.2	13.6	25.4	27.9	25.9	11.2
4	12.5	11.6	18.0	22.9	25.8	10.2
5	15.4	11.1	26.3	26.6	21.0	10.0

Number of Hops

As shown in Table 17, we have calculated the number of hops that a packet has to pass during the simulation assuming shortest path routing algorithm.

Table 17: Number of Hops

Zone	Max	Min	Average	Median
1	18	2	7.23	7
2	15	2	7.23	7
3	20	2	8.12	8
4	20	2	7.71	8
5	15	2	6.85	7

Control Center to Control Center Simulation

Once the data reaches its zonal control center, state estimation is performed for that particular zone. Each zonal control center then sends its information to all the neighboring control centers. Each control center has the static data of system topology for the complete national grid. Control center sometime performs the state estimation using full system topology, local measurements and usually state estimated data from neighboring grid. The problem in just sending the estimated states to the neighboring control center is that the changes in the substation configurations are not reflected in the state estimated data. To take this into account we assume all the measurements from one system to another along with any changes in substation configurations are sent. Hence state estimation at control center can then be performed using local measurements and corrected using system wide measurements. The computation delays in the control center can be of significant importance here.

Currently, the data sharing between control centers is done using Inter Control Center Protocol (ICCP) which is a relatively slow protocol. The data shared between control centers being huge and latency being not the prime concern for EMS application we assumed FTP/TCP kind of traffic. Also it is not suggested to use TCP with UDP as TCP needs to allocate resources on the network before transmission and does get kicked out by UDP. Using TCP helps us in taking care of packet drops because dropping packets is a concern for data collected may be once a second. In communication infrastructure shown in Figure 5, control center shares its information with the all control centers using point to point links. We obtained this network from the location of the zones and by finding shortest path to connect these zonal control centers assuming the optical fiber would run over transmission line. Because there would be only few changes in the system topology over the time, mainly raw measurements results would constitute to the size of the file. The estimated size of the data file time tagged at one particular time is shown in Table 18.

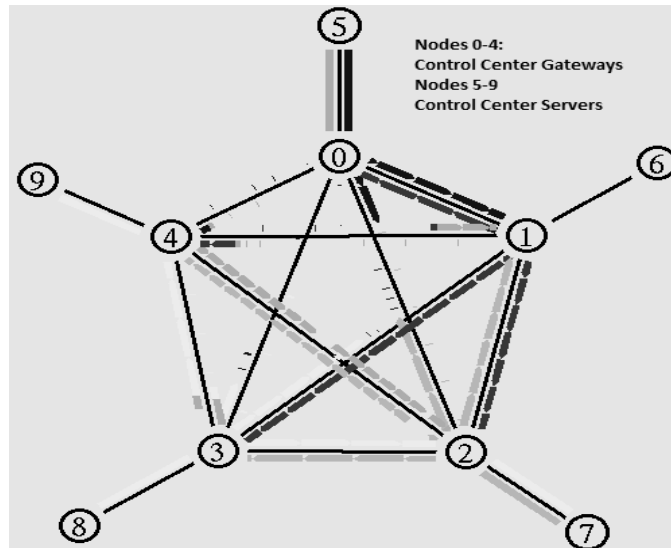


Figure 5: Communication Topology to Connect Control Centers for Polish System

Table 18: File Size of Raw Measurements and Breaker Status

Zone	File size (bytes)
1	99712
2	78514
3	220758
4	144842
5	78748

In Table 19 we have shown that delays to send a complete chunk of file from one control center to another varies as we vary link bandwidth.

Table 19: Delay for Inter Control Center Communications

Bandwidth for CC to CC links (Mbps)	Delay in CC to CC communication	
	Maximum (ms)	Average (ms)
25	118.4	69.1
50	84.3	46.3
75	71.1	39.2
100	65.5	35.5

Based on our understanding for delays in inter control center communication we assumed 50Mbps bandwidth and then calculated total delays shown in Table 20. These delays represent maximum total delay for packets tagged at time $t=0$ to get distributed to all the control centers. Notice that at the control center separate files of raw measurements with different time tags are created. For state estimation purpose one file can be picked up and transmitted every one second.

Table 20: Delay in Exchanging Complete Information Across Polish System

Zone	Max delay for type-1 traffic (ms)	Max CC to CC delay (ms)	Total delay (ms)
1	12.4	66.5	78.9
2	12.7	65.0	77.7
3	14.2	50.8	65.0
4	12.5	61.3	73.8
5	15.4	84.3	99.7

3.3.6. Conclusions

The work presented here provides a basis for simulating the performance of communication network for Power Systems. In this paper a method is developed to determine the parameters to simulate a communications system for a power grid starting from the pow-

er network configuration and the knowledge of the measurement data and the on-line applications. In designing the smart grid infrastructure for a particular power system, the assumptions should reflect the actual design parameters of the communication infrastructure. Such a simulation tool can be used to develop, design and test the performance of the communication system.

We believe that given the actual applications and their precise data requirements further improvements in the results can be obtained on a case to case basis. For example further reduction in bandwidth and latency is possible by using multicast routing and packet tagging. In another scenario we may not send all the traffic to the control center and SPS's can be used as the distributed data bases. Slower EMS applications running in control center can then source the required data from SPSs using middleware architecture like Gridstat. These improvements have to be made based on individual network needs. However, the results in the paper provide us key insight that the average link bandwidth needed for smart grid applications should be in the range of 5-10 Mbps within one control area and 25-75 Mbps for inter control center communications. Using meshed topology delays can be contained within the 100ms latency requirement satisfying all applications. Also with packets traversing just 8-10 hops processing delays at routers should not be a problem.

4. Hierarchical Coordinated Control of Wind Energy Resources and Storage for Electromechanical Stability Enhancement

4.1 Objectives and Methodology

This component of the work seeks to develop control methodologies and designs that optimally mix non-synchronous, variable generation sources such as wind and photovoltaic, with electrical energy storage resources, such as batteries, supercapacitors, and flywheels. It will address the problem of maintaining grid electromechanical stability as the percentage of power production from synchronous generators, the traditional grid stabilizing mechanism, expected to decrease in the coming decade.

4.2 Context and Significance of this Research

The impact of increasing penetration of renewable energy sources on electric grid electromechanical stability is a topic of growing concern in power engineering practice, and has motivated study of improved control designs for alternative energy sources such as wind. Present U.S. grid interconnection standards for wind and photovoltaic electric resource converters largely excuse these generators from responsibility for grid electromechanical stability. As the penetration of wind is expected to grow dramatically in the coming decade, the National Electric Reliability Corporation is predicted to mandate that alternative energy generators contribute to frequency regulation, and possibly to electromechanical stability, for grid reliability.

Most approaches proposed to date seek to make power electronic coupled generation mimic the inertial response of traditional, direct-grid-connected synchronous generators. Indeed, some wind turbine vendors have begun to promote such inertial mimicking capabilities in their advertising.

While the idea of inertial emulation is intuitively appealing, it fails to account for key limitations inherent in attempting to replicate a law of physics with an engineered feedback control, and fails to exploit potential for improved performance through wide area communications.

In traditional, direct-grid-coupled synchronous generators, the effect of inertia has infinite bandwidth and has no actuation limit (though other engineering limits may constrain achievable acceleration/deceleration). In contrast, active control designed to mimic inertia will inevitably be limited both in bandwidth, and in the magnitude of torque or power change that can be applied.

Moreover, inertial response is inherently a single-input/single-output response limited to the local frequency measurement, and cannot respond optimally to stabilize wide area oscillations.

The solution proposed here seeks to examine optimal stability enhancing control designs in a complementary fashion across a range of new generation and storage technologies. Each resource is viewed as an “actuator” channel within a multi-input, multi-output (MIMO) system wide response model. As a key application example, this approach

would complement the control available directly from a wind generator with that available from energy storage devices, such as batteries, flywheels, or supercapacitors. The premise is that it will be typical for energy storage devices to offer relatively fast control action (high bandwidth), while being constrained within relatively narrow limits on the magnitude of power and energy that can be supplied or absorbed.

In contrast to power variation available from energy storage would be changes in electrical power delivery achieved by varying the mechanical shaft power of a wind turbine. For these forms of power control on the turbine itself, it is critical to limit the requested power output changes to very low bandwidth, to avoid stress that can shorten gearbox and drivetrain life.

The designs to be pursued here will develop coordinated MIMO control at a systems level that exploits this complementary relation between the bandwidth and saturation limits among the available “actuators,” while respecting communication bandwidth and latency constraints across the network. This work will extend methodologies for saturation analysis introduced in the control theoretic research literature to treat the practical concerns of optimally tailoring the contribution from each class of controller in the grid (e.g., wind generator, versus energy storage device, versus traditional synchronous generator/turbine set). Constraints on gearbox mechanical stress in wind turbines provide one application in which bandwidth shaping will be critical to reliability and longevity of hardware. At faster timescales, there is anecdotal evidence to suggest that length-of-life for advanced battery technologies may also be influenced by the bandwidth of electrical excitation during charge/discharge. The practical result of such improved control designs will be to increase penetration of grid-connected renewable energy sources, while enhancing electromechanical grid stability as well as equipment life for wind turbines and battery technologies.

Electricity grids around the globe are evolving towards structures that seek to provide dynamic control contributions from non-traditional, non-generation technologies. In the United States, this trend is driven in part by elements of Federal Energy Regulatory Commission (FERC)’s Order No. 890, regarding provision of regulation and frequency services by non-generating resources, and reflected in such implementations as the ISO New England’s Alternative Technology Regulation Pilot Program. In light of this trend, work here develops control algorithms tailored to distributed energy storage units, seeking to use such units to contribute to frequency regulation and to enhance stability of electromechanical modes in the grid. It provides designs that respect saturation limits on power and energy delivery that will be inherent in storage technologies such as batteries, while taking advantage of their capability of varying power output at higher bandwidth than achieved by traditional generators’ governor feedback. Key to the method is a distributed, “modal-focused” approach to feedback controller construction. In particular, regulation and stability enhancement responsibility is spread among the distributed controllers, with a given controller being designed to damp a small subset of the system’s oscillatory electromechanical modes.

Among the goals of the smart grid is that of allowing load resources to contribute to grid control. This contrasts with the traditional utility perspective, that tended to treat load as an uncontrolled, exogenous input, and concentrated all control effort to balance load variation on large-scale, central generators. As the grid comes to rely more on alternative en-

ergy resources such as wind and solar, the traditional utility view may come to be reversed: (some) generators will contribute stochastically varying power along with uncontrolled loads, while responsive load is controlled to help compensate for this stochastic input, and thereby regulate frequency. This goal will be facilitated by the growth of cost effective distributed storage technologies, such as batteries, as these interface to the grid at the substation and even consumer load level. Plug hybrid electric vehicles have received the most notice as harbingers of this distributed storage technology, but a number of types of test installation for battery storage are beginning to appear [34]. Regulatory recognition of this trend is reflected in actions by FERC [31], in the ISO New England’s Alternative Technology Regulation Pilot Program [32].

The premise of the work here is that such use of distributed storage for frequency regulation and grid stabilization will require a new class of distributed control algorithms. The performance of such control will be greatly enhanced if the designs explicitly recognize the saturation limits on power and energy delivery that are inherent in storage technologies such as batteries, while taking advantage of their capability of varying power output at higher bandwidth than achieved by traditional generators’ governor feedback. Key to the design method will be a distributed, “modal-focused” approach to local observer and feedback controller construction that is well-suited to the nature of power grid electromechanical dynamics. In particular, regulation and stability enhancement responsibility is spread among the distributed controllers, with a given local device being designed to observe and damp a small subset of the system’s oscillatory electromechanical modes.

4.3 A Hierarchical Multi-input/Multi-output Design Method

The authors of Saberi [33] have demonstrated an optimal control design method to form controller design in the context of linear systems with elements subject to input amplitude limits (e.g., actuator saturation). The objective is output regulation in the face of disturbances characterized by an exosystem, where the exosystem is explicitly constructed as part of the overall model. In many ways, this framework is particularly well suited to the frequency regulation problem in the power systems context, and allows treatment of power and energy limits that are critical to the successful incorporation of distributed energy storage technologies. We recall their “low- high gain” design method that yields a family of state feedback gains, parameterized in a low gain parameter, q , and a high gain parameter, μ . Consider the linear system:

$$\dot{x} = Ax + B\sigma(u) + E_w w \quad (1)$$

$$\dot{w} = Sw \quad (2)$$

$$y = Cx + D_{yw} w \quad (3)$$

Equation (1) describes the plant with state $x \in \mathbf{R}^n$ and control input $u \in \mathbf{R}^m$, subject to the effect of an exogenous disturbance represented by $E_w w$ where $w \in \mathbf{R}^s$ is the state of an exosystem. Equation (2) describes the state space realization of the autonomous exosystem, typically constructed to produce periodic disturbance signals (i.e., S will typically be selected to have purely complex conjugate pair eigenvalues representing the disturbance

signals' spectral content). The output is $y \in \mathbf{R}^p$, and σ is a normalized vector-valued saturation function defined as:

$$\sigma(s) = [\bar{\sigma}(s_1), \bar{\sigma}(s_2), \dots, \bar{\sigma}(s_m)]^T \quad (4)$$

$$\bar{\sigma}(s) = \begin{cases} s & \text{if } |s| \leq 1 \\ -1 & \text{if } s < -1 \\ 1 & \text{if } s > 1. \end{cases}$$

This system representation is largely linear, save for the presence of the saturation function, σ , which introduces non-linearity that has impact only if the control signal input exceeds the saturation threshold. If all the eigenvalues of A lie in the closed left-half plane and the pair (A, B) is stabilizable, then one may consider a linear state feedback, designed by solving the algebraic Riccati equation:

$$P_\epsilon A + A^T P_\epsilon - P_\epsilon B B^T P_\epsilon + Q_\epsilon = 0 \quad (5)$$

where, $Q_\epsilon: (0, 1] \rightarrow \mathbf{R}^{n \times n}$ is a continuously differentiable matrix-valued function such that $Q_\epsilon > 0$, $\partial Q_\epsilon / \partial \epsilon > 0$ for any $\epsilon \in (0, 1]$, and $\lim_{\epsilon \rightarrow 0} Q_\epsilon = \mathbf{0}_{n \times n}$. The solution to (5) is a unique positive definite P_ϵ that is continuously differentiable with respect to ϵ , is monotonically increasing with ϵ , and $\lim_{\epsilon \rightarrow 0} P_\epsilon = \mathbf{0}_{n \times n}$. Then, the state feedback gain matrix $F_{\mu, \epsilon}$ is given by:

$$F_{\mu, \epsilon} = -(\mu + 1)B^T P_\epsilon \quad (6)$$

where, μ is the high gain control parameter, ϵ is the low gain parameter. The feedback control law is given by:

$$u = F_{\mu, \epsilon} x + [\Gamma - F_{\mu, \epsilon} \Pi] w \quad (7)$$

Feedback using $F_{\mu, \epsilon}$ yields an asymptotically stable undisturbed system for any $\epsilon \in (0, 1]$. As sufficient conditions to ensure regulation in the presence of the exosystem's disturbance signal, w , there should exist matrices Π and Γ that solve the regulator equation:

$$\Pi S = A \Pi + B \Gamma + E_w \quad (8)$$

$$0 = C \Pi \quad (9)$$

Moreover, for any allowable initial condition on the exosystem, there must exist $\delta > 0$ and a time $T \geq 0$ such that $\|\Gamma w\|_{\infty, T} \leq 1 - \delta$. For the class of exosystem to be employed here, that is simply a set of undamped second order oscillators with integer multiple frequencies (i.e., basis functions for a truncated Fourier representation of a periodic disturb-

ance signal), the set of allowable initial conditions on the exosystem state can be taken as a norm ball. In this scenario, the condition $\|\Gamma \mathbf{w}\|_{\infty, T} \leq 1 - \delta$ is guaranteed satisfiable if a sufficiently small norm ball of initial conditions is selected; i.e., the magnitude of the disturbance signal is controlled by the size of its initial condition set. Hence, one intuitive measure of the quality of the control design here can be judged as follows: how large a disturbance magnitude can the system regulate, without exceeding the saturation limits on the actuators. Note that the regulator equation to identify Γ and Π above can be solved using standard techniques for linear matrix equations.

Following the philosophy of [33]'s low-high gain method, in [35]-[38] the authors of this work offer an enhancement, to more fully utilize the available control power when one has actuators of differing saturation limits and bandwidth. In particular, in this paper two classes of actuators are considered: one for which the actuators have broad saturation limits but low bandwidth (conventional governor control systems) and other for which the actuators have low saturation limits but high bandwidth (batteries). A modal coordinate system is adopted, and control effort is reserved for a subset of system modes. In practical terms this subset of modes of concern corresponds to lightly damped electromechanical modes likely to be excited by the disturbance signal. This modal partitioning also allows the complementary nature of saturation limits and bandwidth limits of actuators to be better exploited.

The input channels can be partitioned according to the bandwidth of the corresponding actuators. Let p_1 be the input channels that consist of the high bandwidth actuators and p_2 be those consisting of the low bandwidth actuators. Let \mathbf{A}_{net} , \mathbf{B}_{net} , \mathbf{C}_{net} denote the state space representation of the system (including the power system and the actuators). The details follow in the next section. To partition the \mathbf{Q}_e matrix consistent with the partitioned input channels, the system is transformed into its modal co-ordinates. The transformation square matrix \mathbf{P}^{-1} is formed, such that every real eigenvector, \mathbf{q}_i , of the matrix \mathbf{A}_{net} forms a single column of \mathbf{P}^{-1} , and every complex eigenvector of \mathbf{A}_{net} , \mathbf{q}_j , yields two columns in \mathbf{P}^{-1} with one column the real part of \mathbf{q}_j and the other column the imaginary part of \mathbf{q}_j . The state matrix in the modal coordinate frame is given by:

$$\bar{\mathbf{A}}_{\text{net}} = \mathbf{P} \mathbf{A}_{\text{net}} \mathbf{P}^{-1}$$

The matrix $\bar{\mathbf{A}}_{\text{net}}$ thus formed has all the real eigenvalues of \mathbf{A}_{net} on the diagonal, and each of the complex eigenvalues result in blocks of size 2×2 with the real part of the eigenvalues on the diagonal and the imaginary part appearing as skew symmetric terms on the off-diagonal.

The modal degrees of controllability with respect to each of the input channels are of interest, so that the states can be partitioned according to the corresponding partitions of input channels. For each input channel, i , and each mode of the system, k , the scalar, $m_{i,k}$, given by:

$$m_{i,k} = |\mathbf{w}_k^T \mathbf{b}_i| \quad (10)$$

is formed. Where, \mathbf{w}_k is the normalized left eigenvector of $\bar{\mathbf{A}}_{\text{net}}$ in the modal form corre-

sponding to the mode k ($\|\mathbf{w}_k\| = 1$), \mathbf{b}_i is the i^{th} column of \mathbf{B}_{net} in the modal form. This gives blocks of 2 states which are most controllable for each of the input channels.

Using this information, the corresponding diagonal blocks of the \mathbf{Q}_ε matrix parameterized in two different ε 's can be partitioned. The ε 's are chosen such that a higher value of ε is chosen for the blocks corresponding to the higher bandwidth input channels.

4.4 The System Model

In this section the state space model of the system is developed. The system consists of three components: the electric power network, the actuators (energy storage devices and governor control systems), and the exosystem (to model load variations). We describe briefly the construction of each of these components and then form the net system model.

4.4.1. Modeling Power Injection Variation Disturbances to be Regulated

The frequency regulation problem in the power grid is fundamentally tasked with maintaining area wide power balance, which is then reflected in the degree to which frequency is regulated to the desired 60 or 50 Hz set-point. In the power systems context, this control objective is partitioned across several time scales, the fastest of which is termed “primary” frequency control. Hence, on this “primary” time scale, the key disturbance signal of interest is the fast variation in load (perhaps 100’s of milliseconds to 10’s of seconds), about its longer term and more predictable diurnal variation. In general, one would seek to characterize the spectral content of the load variation of interest, and reproduce this spectrum in the frequencies of the imaginary eigenvalues of the matrix \mathbf{S} . Here the exosystem is constructed with state matrix \mathbf{S} , governing the dynamics of the exosystem according to (2), chosen such that it has purely imaginary pairs of eigenvalues. With an appropriate choice of initial conditions, \mathbf{w}_0 , this unforced system produces an output that approximates a periodic square wave can be constructed. More specifically, a \mathbf{S} matrix of size 10×10 , given by:

$$\mathbf{S} = \begin{bmatrix} 0 & 1 & & & & & & & & & \\ -1 & 0 & & & & & & & & & \\ & & 0 & 3 & & & & & & & \\ & & -3 & 0 & & & & & & & \\ & & & & & \ddots & & & & & \\ & & & & & & & & 0 & 9 & \\ & & & & & & & & -9 & 0 & \end{bmatrix} * \omega_s$$

is chosen, where ω_s is the frequency of the periodic square wave. For the specific initial conditions of:

$$\mathbf{w}_0 = 0.02 * [0 \quad 1 \quad 0 \quad 1 \cdots 0 \quad 1]^T$$

direct calculation confirms that $\omega(t)$ trajectories will contain sinusoids at ω_s and its odd harmonics to order 9, with the amplitude of $\omega(t)$ equal to 0.02 (indicating that load varia-

tions with an amplitude of 0.02 are considered here). The matrix E_ω is chosen such that each row, $E_{\omega,i}$, corresponding to each varying load, i , is of the form:

$$E_{\omega i} = \left[\frac{1}{1} \quad 0 \quad \frac{1}{3} \quad 0 \cdots \frac{1}{9} \quad 0 \right].$$

The remaining rows of E_ω are set to zero, so that the periodic square wave affects only the varying loads.

4.4.2. The IEEE 14 Bus Test System

The IEEE 14 bus test system represents a 14 bus power system with 5 generator buses and 9 load buses. Buses numbered 1, 2, 3, 6 and 8 represent the generator buses. The other buses represent the load buses. The state space formulation of this system is assembled as follows.

The electromechanical behavior of each of the generators in the system can be captured by standard swing equation models [39]. The frequency,¹, and the angle, δ , are by definition related as:

$$\Delta \dot{\delta} = \Delta \omega \quad (11)$$

The differential equation governing the dynamics of the generator, typically termed the “swing equation,” is given by:

$$M \Delta \dot{\omega} = P_m - P_e - D \Delta \omega \quad (12)$$

where, M represents the normalized rotational inertia of the generator, D the damping constant, P_m the mechanical shaft power input to the generator, P_e the electrical power output absorbed by the network from the generator.

P_e must also balance the power absorbed by the rest of the network at the generator bus and is related to the other network variables through the standard power flow equations. The loads in the network are modeled according to the standard structure preserving dynamic model presented in [40]. The network equations are inherently non-linear in nature. As is typical in power systems practice, the feedback control design is based on a linearization about the operating point.

A state space model of the linearized 14 bus system with the $\Delta \omega$'s and $\Delta \delta$'s of each of the generators, $\Delta \delta$'s of each of the loads as states is formed. The inputs to the system are the mechanical input powers, P_m , for the generating units, and the load variations. A state space representation of the system similar to the one described by (1) and (3) can be formed.

4.4.3. Modeling of the Actuators

The actuators considered for this problem lie in two distinct classes: the batteries that have high bandwidth but low saturation limits, and the governor control systems at the

synchronous generators' locations that have low bandwidth but high saturation limits. The modeling of these actuators is described below.

Batteries: A 2-capacitance model presented in [41] is considered here to represent lithium-ion batteries that might be typical in hybrid electric vehicles. The model is a second order R-C circuit model, such that it behaves like a high pass filter, thereby limiting the DC gain to a very small value.

Governor control systems: The governor control systems at each of the generator locations can be modeled with standard first order blocks. Standard transfer functions for such systems from [39] are adopted in this paper. The overall state space model composed of the actuators and the 14 bus test system (plant) is formed as follows. The states of the net system are given by:

$$\Delta x_{net} = \begin{bmatrix} \Delta x_{act} \\ \Delta x \end{bmatrix} \quad (13)$$

The state equations defining the actuators are:

$$\Delta \dot{x}_{act} = A_{act} \Delta x_{act} + B_{act} \Delta u_{act} \quad (14)$$

$$\Delta y_{act} = C_{act} \Delta x_{act} + D_{act} \Delta u_{act} \quad (15)$$

The input to the plant is the output of the actuators as shown in Figure 6. Thus:

$$\Delta e = C_{act} \Delta x_{act} + D_{act} \Delta u_{act} \quad (16)$$

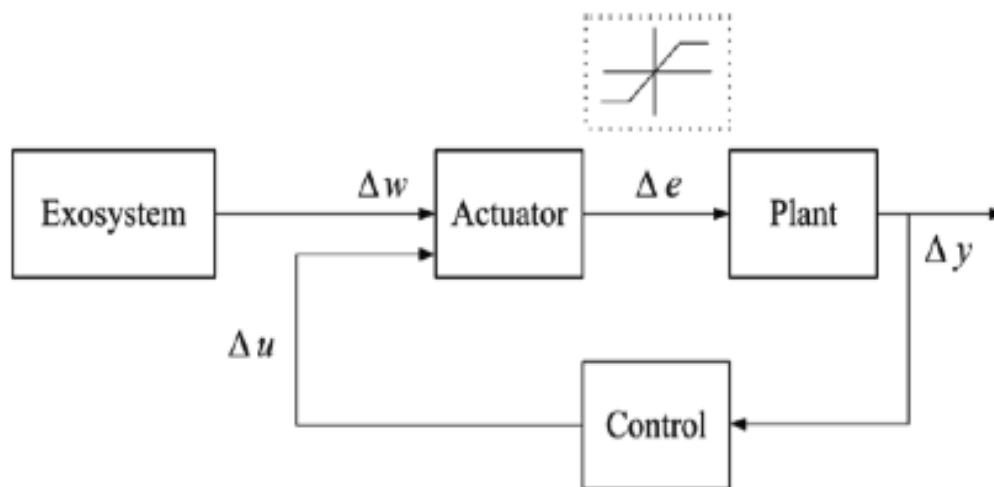


Figure 6: Conceptual Block Diagram Illustrating Exosystem Role

The resulting system consists of 33 states (14 actuator states, 19 power network states) and is given by:

$$\Delta \dot{x}_{net} = A_{net} \Delta x_{net} + B_{net} \Delta u + E_w \Delta w \quad (17)$$

$$\Delta y = C_{net} \Delta x_{net} \quad (18)$$

where:

$$A_{net} = \begin{bmatrix} A_{act} & \mathbf{0} \\ BC_{act} & A \end{bmatrix} \quad (19)$$

$$B_{net} = \begin{bmatrix} B_{act} \\ BD_{act} \end{bmatrix} \quad (20)$$

$$C_{net} = [DC_{act} \quad C] \quad (21)$$

4.4.4. Implementation of the Control Design

A scenario where the loads at buses numbered 4 and 5 vary periodically is considered. The batteries are connected at the load buses numbered 10 and 14. The governor control systems are connected at all the generator buses (buses numbered 1, 2, 3, 6 and 8). Then, the low-high gain design method is applied to this case. Denoting p_1 as the set of channels with high bandwidth (batteries) and p_2 as the set with lower bandwidths (governors). Let $\Delta e_1(t)$ and $\Delta e_2(t)$ represent the control power signals for each of these partitioned channels p_1 and p_2 respectively. Choosing $\varepsilon_1 = 1 \times 10^{-6}$ and $\varepsilon_2 = 1 \times 10^{-1}$, the quantities $\|\Delta e_1(t)\|$ and $\|\Delta e_2(t)\|$ can be examined for the corresponding partitions (call this the nominal case). From Figure 8 it can be seen that for the battery channels, p_1 , the norm of the control signals is much less than that for the governor channels, p_2 . The average values of $\|\Delta e_1(t)\|$ and $\|\Delta e_2(t)\|$ are 6.8×10^{-7} and 7.6×10^{-5} respectively. The ratio of these average values is 112. The power system is required to operate at a single common frequency in equilibrium. It is therefore useful to examine a weighted sum of all the generator frequencies to see the effect of the controller on system frequency. Consider the weighted sum:

$$\Delta y_{out} = \frac{\sum_{i=1}^5 (\Delta y_i H_i)}{\sum_{i=1}^5 H_i} \quad (22)$$

Where, H_i is the inertia of the generator i in seconds. The resulting plot of this output is shown in Figure 9. To illustrate the effectiveness of this control method, we show the performance of the open loop system (i.e., the system with the IEEE 14 bus test system

and actuators, but without the state feedback). We assume that the saturation limit on the output power of the batteries is quite small, at 1.5×10^{-5} p.u., relative to the IEEE 14 bus system's base of 100 MVA. Furthermore, in order to illustrate a scenario where the output powers could go beyond the saturation limits, the amplitude of load variation is increased from 0.02 to 0.3. Then, for the open loop system, the resulting battery output signals, $\Delta e_{11}(t)$ and $\Delta e_{12}(t)$, are shown in Figure 10. It is clear from the figure that in certain intervals of time, the battery signals reach the saturation limit. The resulting $\|\Delta e_1(t)\|$ and $\|\Delta e_2(t)\|$ are shown in Figure 11. It can be seen that in order to regulate the frequency changes due to this larger amplitude of load variation, the governors have to operate at a very fast rate and this may not be practically feasible. The resulting output is shown for this scenario, with the same $\varepsilon_1, \varepsilon_2$ values as earlier. The resulting $\|\Delta e_1(t)\|$ and $\|\Delta e_2(t)\|$ are shown in Figure 13. From the figure it can be seen that the battery channel signals exceed the magnitude that represent saturation limits, during certain time intervals. The associated Frequency Deviation performance output is shown in Figure 14. In order to ensure that the batteries always operate in their linear regions of operation, the low gain design parameters $\varepsilon_1, \varepsilon_2$ are changed. Choosing $\varepsilon_1 = 1 \times 10^{-5}$ and $\varepsilon_2 = 1 \times 10^{-1}$, the resulting $\|\Delta e_1(t)\|$ and $\|\Delta e_2(t)\|$ are shown in Figure 15. Observing the magnitude reached by the battery signals, from Figure 15 it can be seen that the low-high gain design method results in the batteries operating in their linear regions of operation. The resulting Frequency Deviation performance is shown in Figure 16 below. The individual battery output signals, $\Delta e_{11}(t)$ and $\Delta e_{12}(t)$, for the above two cases are shown in Figures 17 and 18 respectively.

Next, we demonstrate a distributed, observer-based implementation of the control scheme, the details of which are presented in [35]. This scheme utilizes a small subset of available phasor measurement unit (PMU) signals to form estimates of the system states that are then fed to each of the local controllers. In particular, we have observer/controller pairs at each of the actuator locations, i.e., at each of the governor control locations and each of the battery locations. This approach overcomes the limitations of traditional centralized control, where large communication bandwidth is required for exchanging information between various sub-systems. For the IEEE 14 bus test system considered in this work, we look at performance for different sets of measurement signals that would come closest to the full state feedback scheme. A choice of signals where each of the generator bus observers utilize local generator frequency and angle measurement signals, while each of the battery bus observers utilize one remote PMU signal of a generator frequency results in the best performance for a scheme that utilizes a small subset of available PMU measurement signals. The resulting $\|\Delta e_1(t)\|$ and $\|\Delta e_2(t)\|$ are shown in Figure 14. Comparing Figure 19 with Figure 8, it can be seen that the observer-based control scheme, while not quite achieving the ideal of the full state feedback, performs satisfactorily in terms of sharing the control effort between the two classes of actuators.

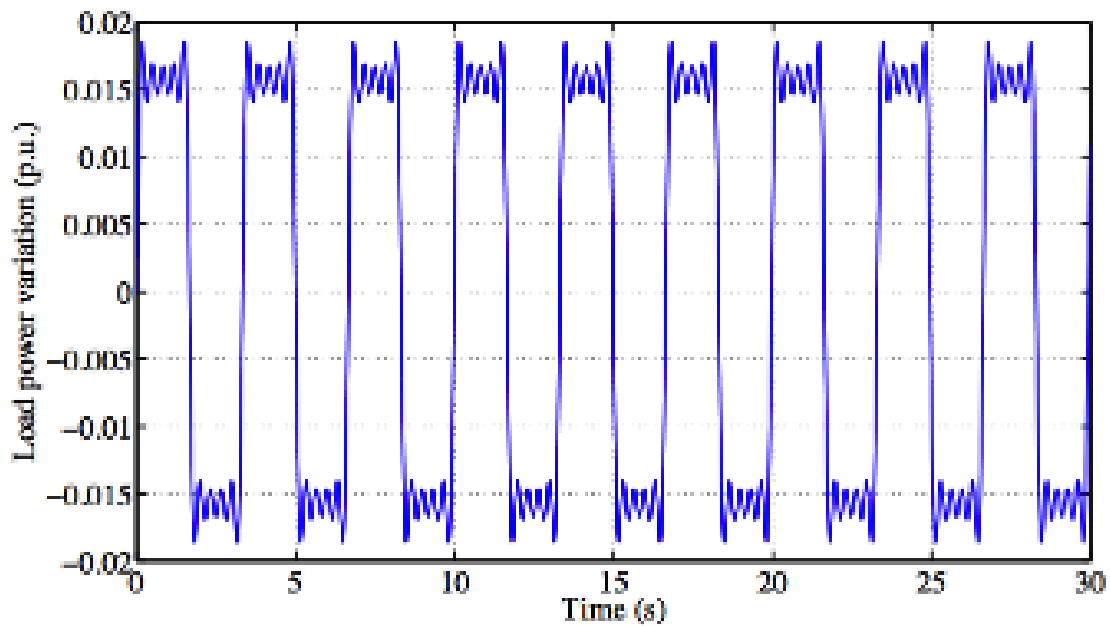


Figure 7: Time Plot of Load Disturbance—Fast Time Scale Periodic Switching Selected as a Representative “Worst Case” Disturbance Against Which Controller Must Regulate

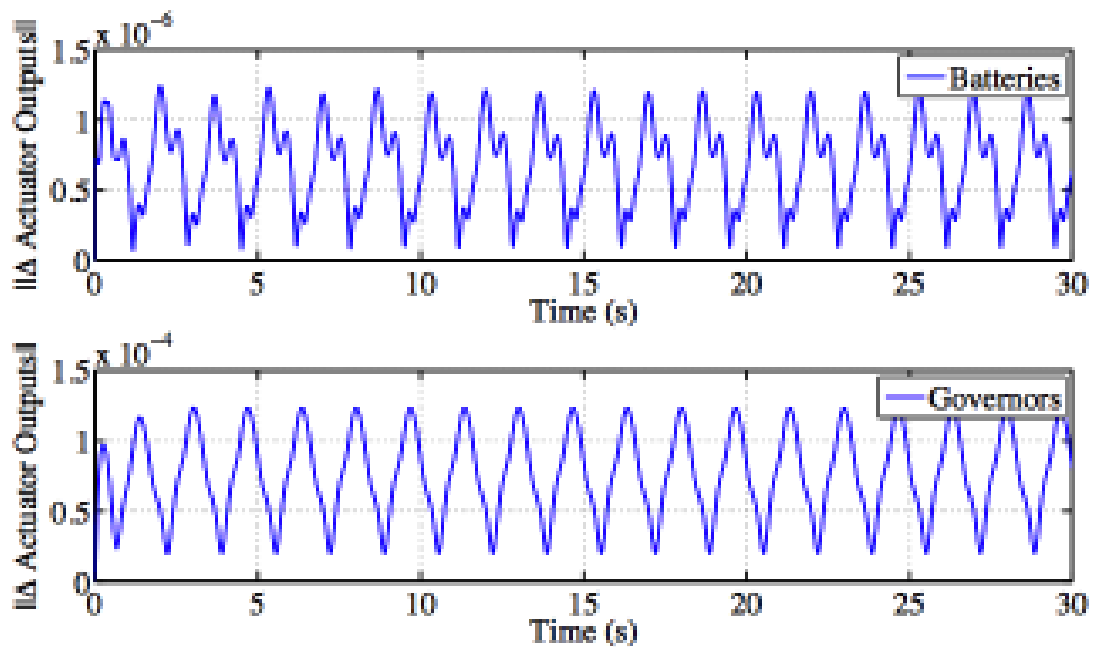


Figure 8: Actuator Signals Nominal Case

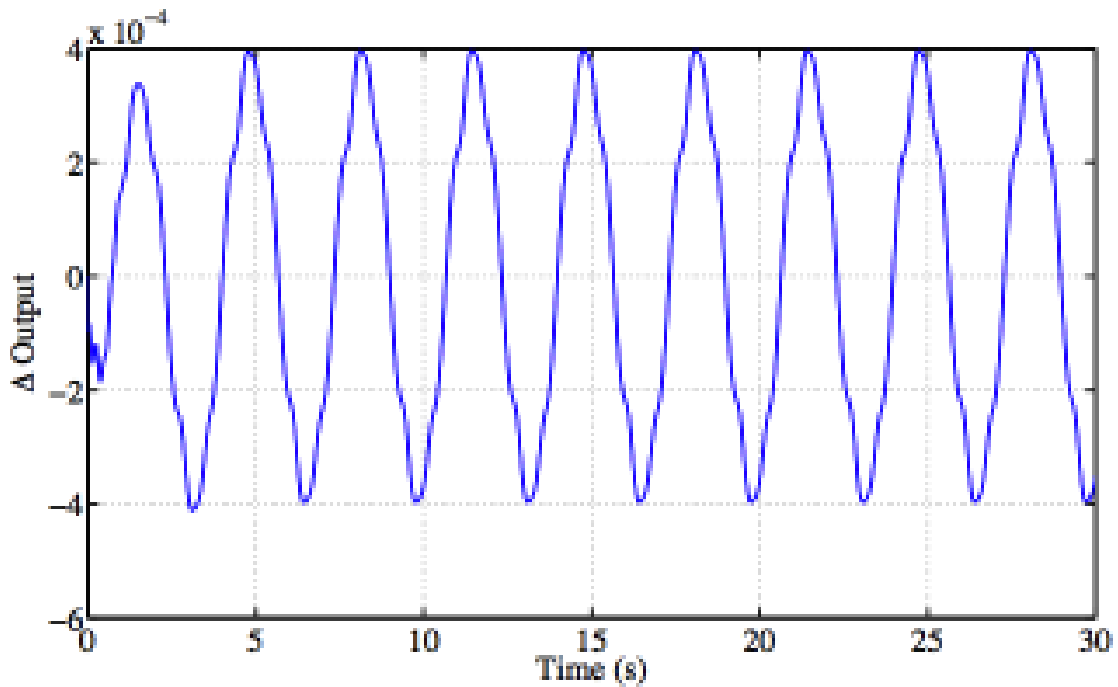


Figure 9: Weighted Output–Nominal Case

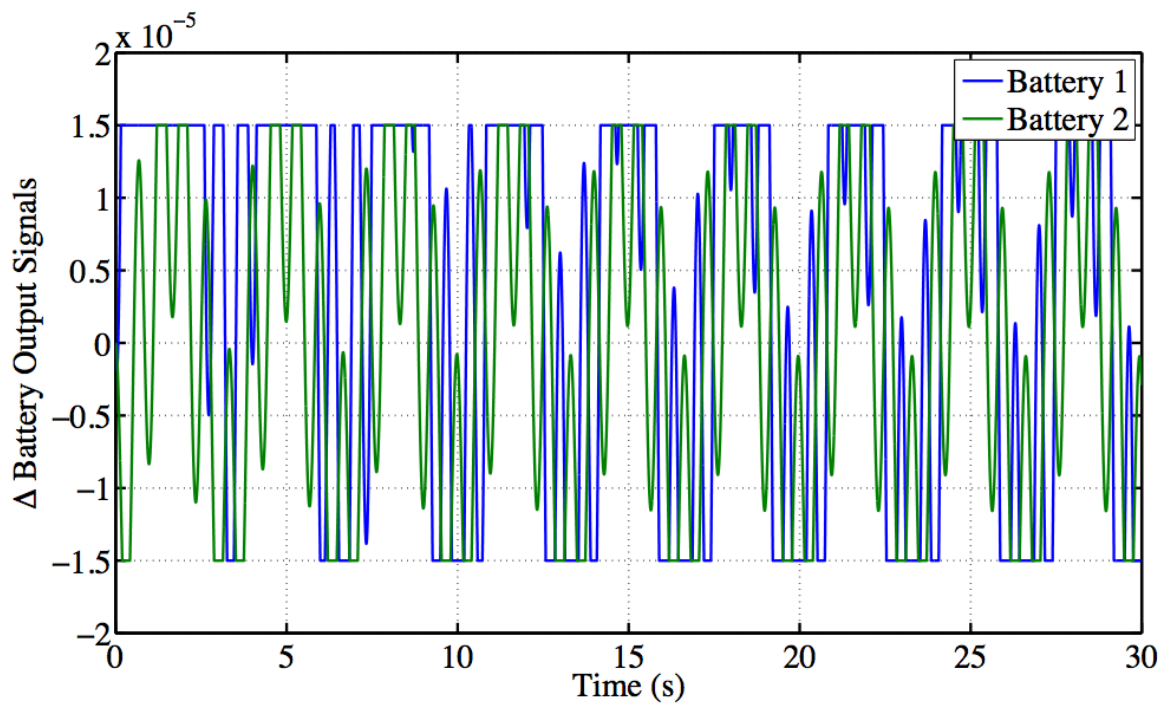


Figure 10: Battery Output–Open Loop Case

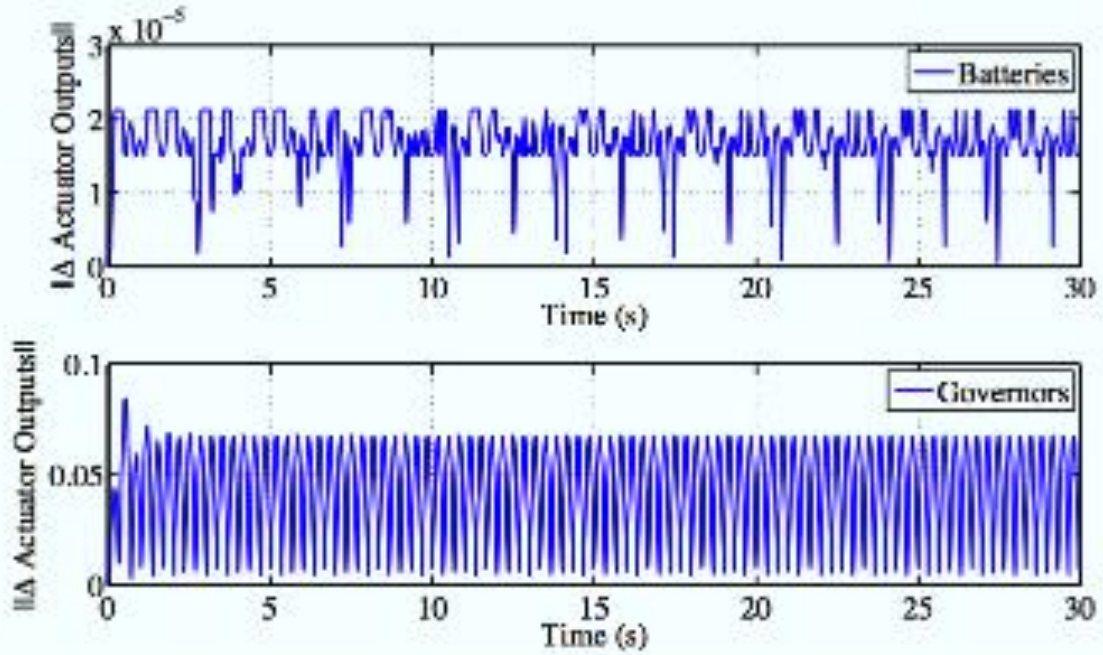


Figure 11: Actuator Signals–Open Loop Case

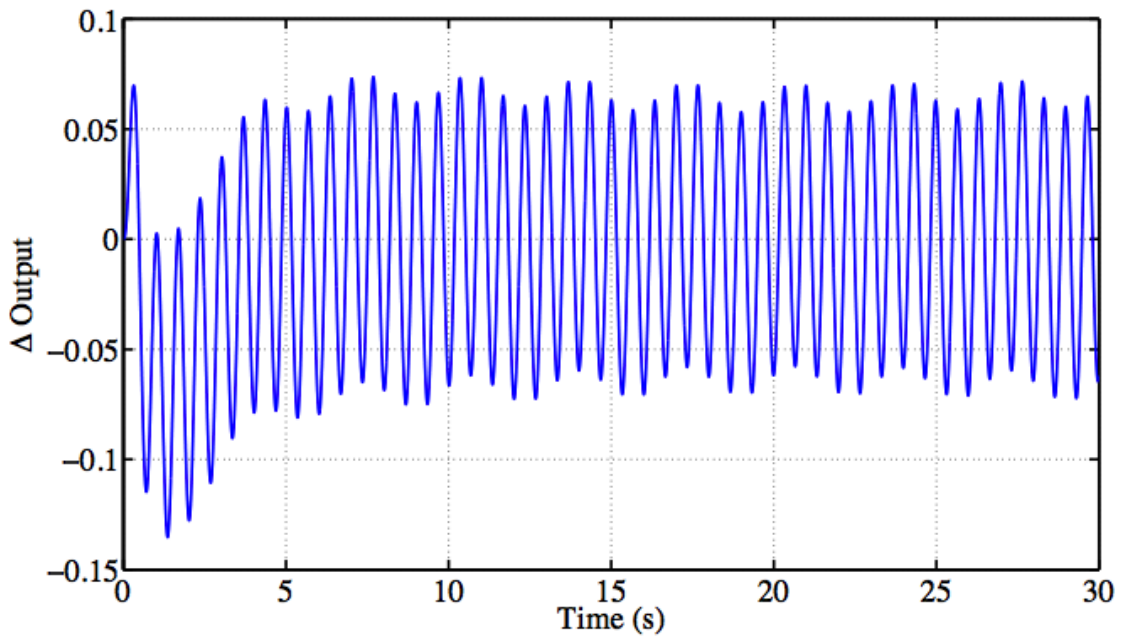


Figure 12: Weighted Output–Open Loop Case

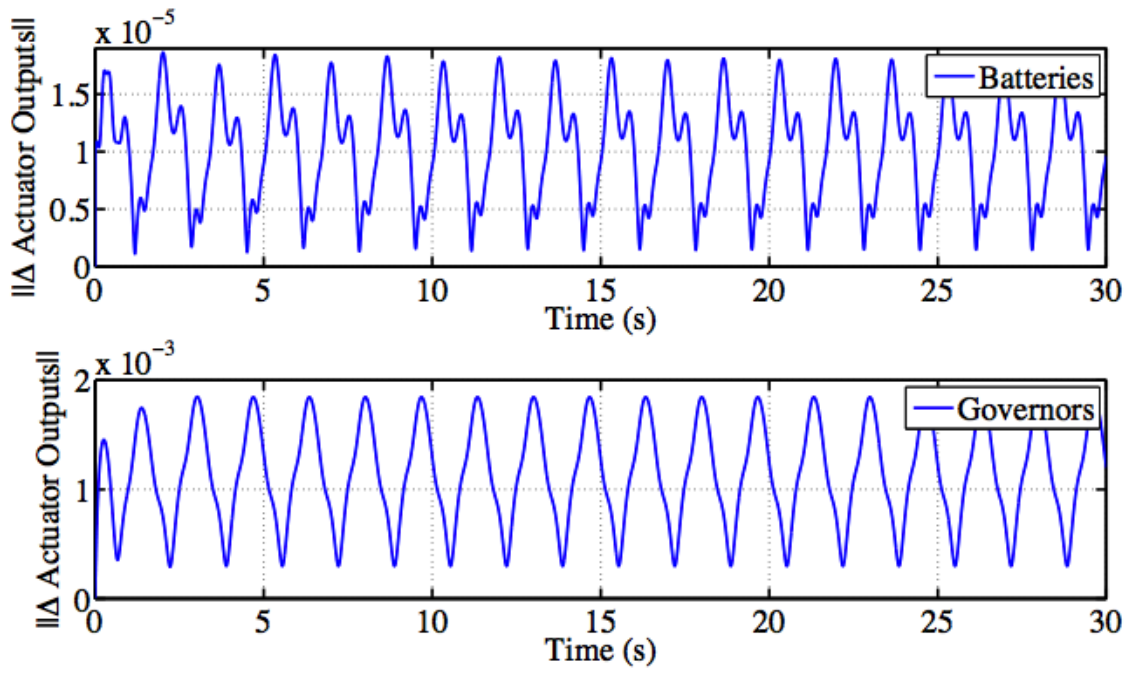


Figure 13: Actuator Signals–Saturation Case

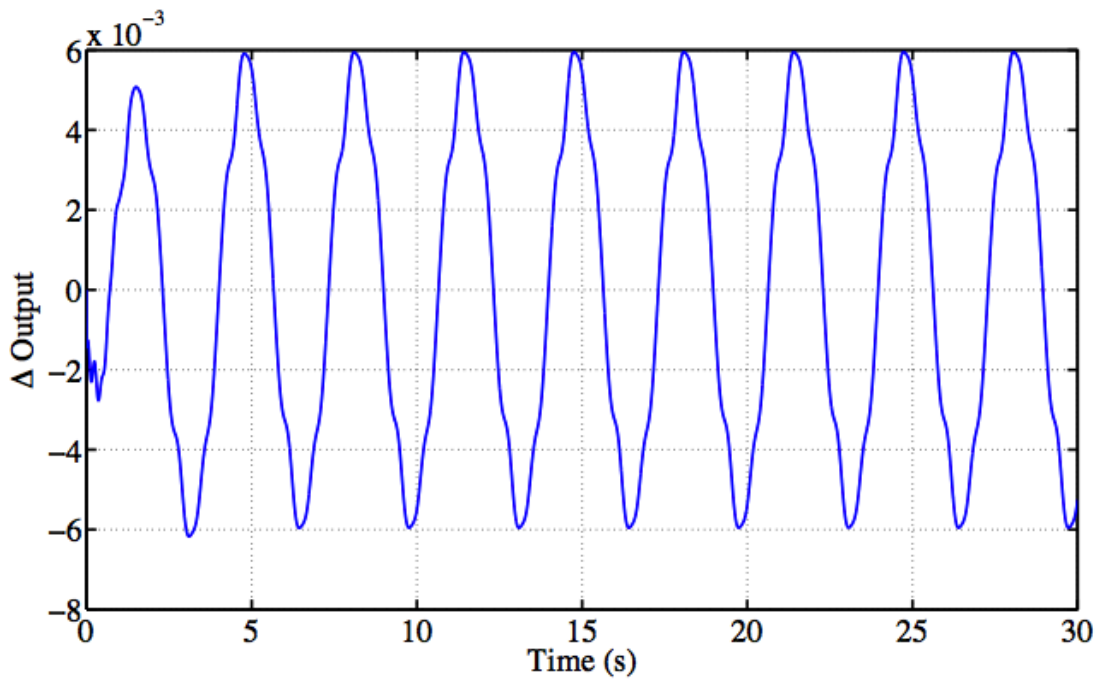


Figure 14: Frequency Deviation Performance–Saturation Case

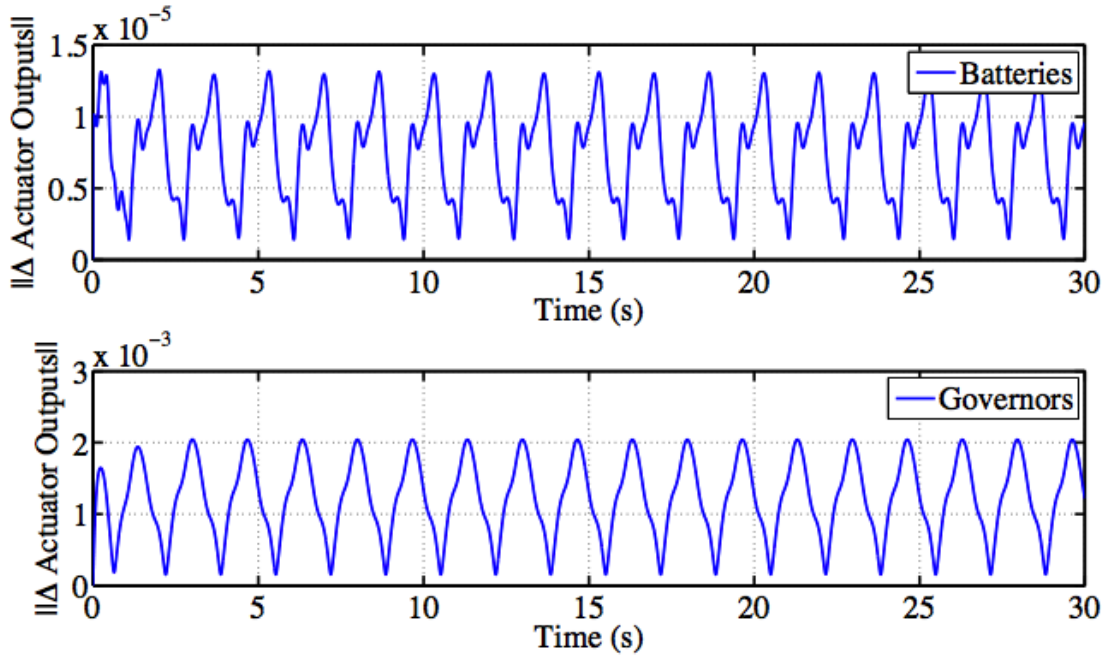


Figure 15: Actuator Signals–Case of Control Design Accounting Saturation

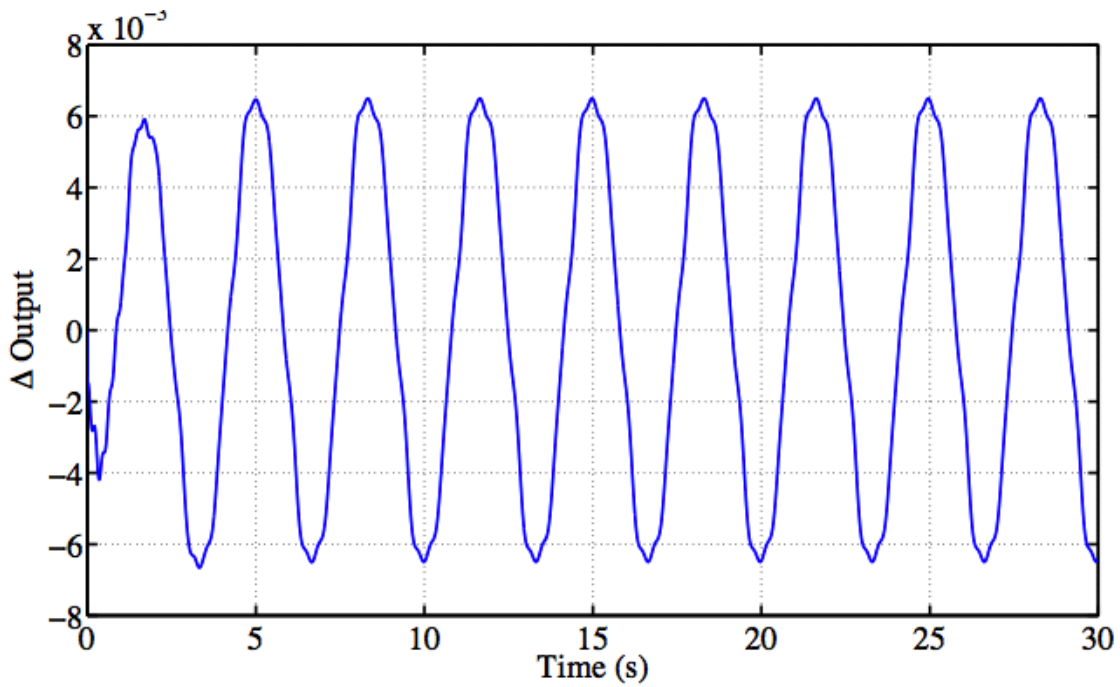


Figure 16: Frequency Deviation Performance–Case of Control Design Accounting Saturation

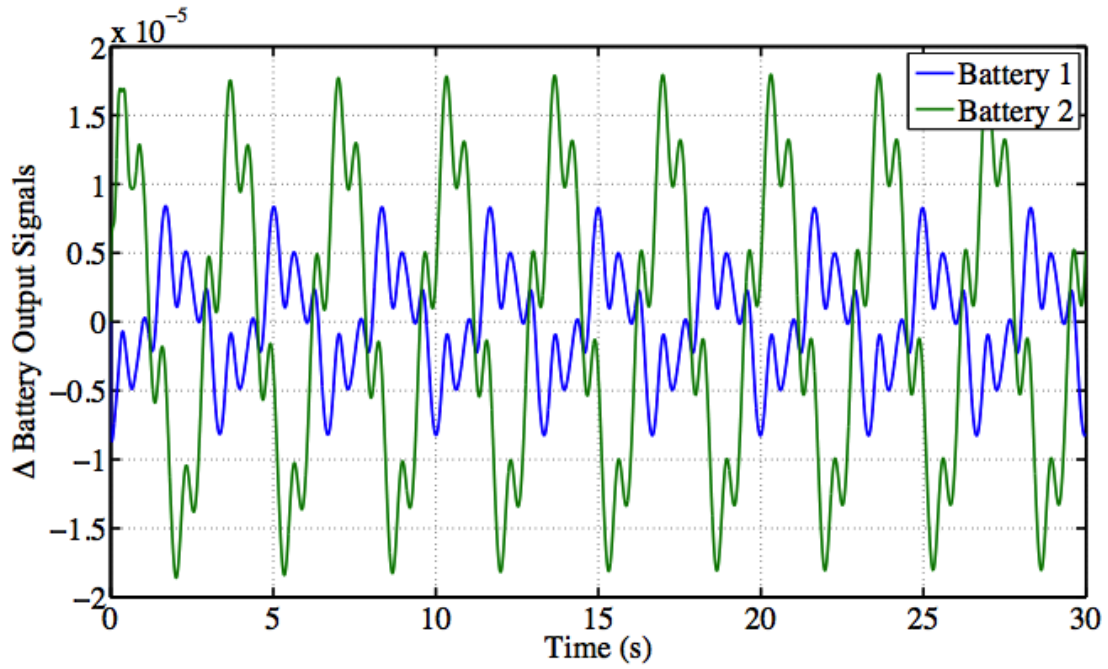


Figure 17: Battery Output Signals–Saturation Case

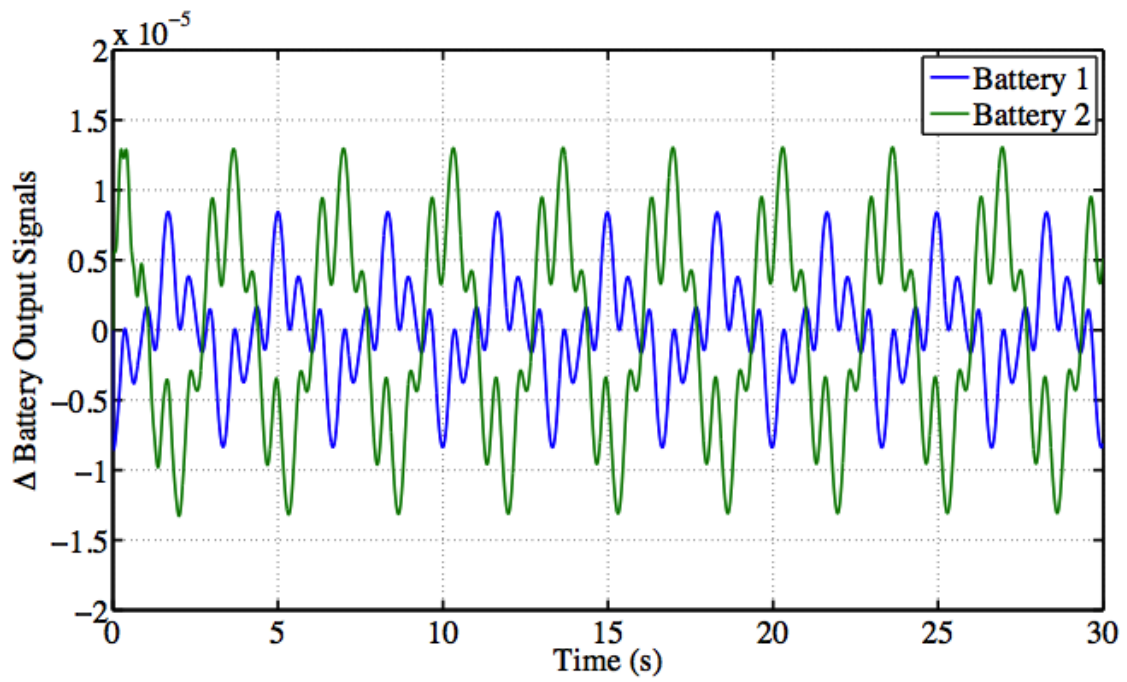


Figure 18: Battery Output Signals–Control Designed to Remain within Limits

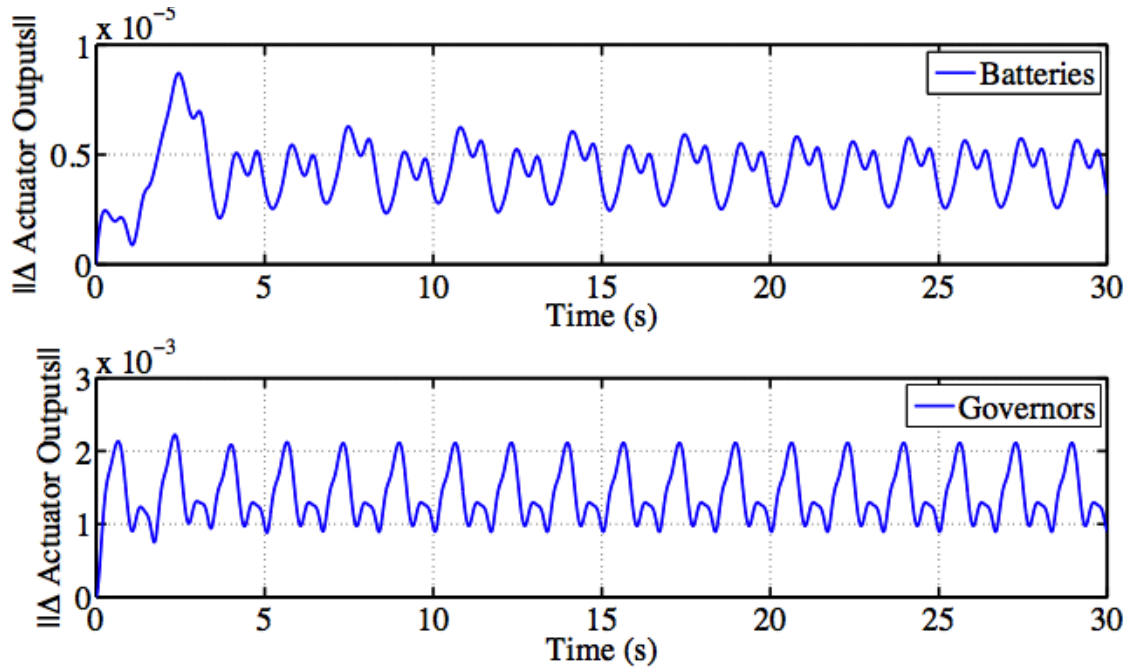


Figure 19: Actuator Signals–Observer Based Scheme

5. Hierarchical Coordinated Protection of the Smart Grid with High Penetration of Renewable Resources

5.1 Objectives and Methodology

New protection paradigm for smart grids is envisioned to be able to deal with the grid behavior that has not been seen before but is anticipated in the future: heavy loading conditions, abrupt changes in generation patterns, extensive switching of power system configuration and high penetration of distributed generation. This will lead to an equal importance of dependability and security of protective relay operations, which is hard to achieve simultaneously since in the past designing protection systems for trade-offs between dependability and security was common. To avoid relay misoperations that may lead to cascades, the new protection methodology takes into account two seemingly unrelated concepts (decentralized component protection and centralized wide area protection) and creates a new integrated concept (hierarchically coordinated protection). The objective is to define the three hierarchical coordinated layers:

- **Predictive Protection:** System conditions leading to major disturbances are recognized through on-line means and local protection is “armed” to respond with specific tripping/blocking logic preventing disturbance from unfolding into a cascade.
- **Inherently Adaptive Protection:** It adjusts its tripping logic based on feature patterns of waveform measurements that are recognized on line and matched to the patterns obtained during learning process that includes thousands of potential fault conditions.
- **Corrective Protection:** If local transmission line protection misoperates, accurate and fast fault location/analysis restores the system component(s) quickly if the original tripping action is determined not to be warranted.

This approach may be utilized at all power system levels and any robust and reliable protection scheme may be defined and developed following these three steps. The methodology is illustrated with real life system scenarios to demonstrate some of the findings.

5.2 Context and Significance of this Research

The present protection schemes are based on principles introduced many decades ago when the power grid was less complex, had high component redundancy and utilized centralized power generation only at the transmission level. In the last decade, the transmission system structure became more complex and operation scenarios changed due to rapid installation of the renewable generation sources and deferral of the grid infrastructure upgrade. The system is planned to operate with tight margins and less redundancy and under dynamic grid operating phenomena such as power and voltage oscillations, as well as voltage, frequency and angular instability. Those phenomena deteriorate system performance and may cause a protection operation malfunction that leads to the system blackouts. The recent blackouts show that existing control cannot handle and detect prop-

agated disturbances, such as cascading events and because of that the relays and protection schemes have to be more accurate and reliable.

Beside this, the power generation has been moved to the distribution level too. In the past, distribution system was characterized as passive network with radial feeders that transfer power in one direction from substation to the customers only. The fuses, recloses and overcurrent relays are used to isolate the faults in the system. They all operate on changes in current magnitude and their logic is based on the assumptions that fault current magnitude is much higher than normal current magnitude and that it decays by distance. However, this might not be the case for the system with high penetration of distributed generation (DG). The DG fault contribution depends of generator technology, and in case of inverter-based type the fault current is significantly lower compared to conventional synchronous machine based generators. Also, interfacing to such DG becomes volatile to voltage dips in the main network and voltage ride through capabilities are required. Similarly, DG introduces bidirectional power flow in distribution system and this may increase or decrease fault current level under different circumstances. Because of all of this, it becomes less possible to protect network using overcurrent relays with predefined settings threshold. The more intelligent relays and protection approaches have to be developed.

The proposed study aims at understanding how the three relaying concepts defined in the objectives are implemented in a hierarchically coordinated way to improve dependability (trip when fault is present) and security (no trip when fault is not present) of the relaying scheme to accommodate increases in network loading, more frequent switching of the topology, and high penetration of renewable and intermittent resources. The proposed approach inherently requires full understanding of not only the advanced technology concepts such as PMUs, intelligent systems, advanced signals processing and communications but also the shortcomings of legacy solutions. It creates training opportunity for developers and users alike to understand how the legacy relaying works, why it fails to offer satisfactory solution for complex network conditions expected in the future, and what are the expectations for professional skills of the future protection engineers needed to cope with existing issues and design new solutions.

5.3 New Architectures for Coordinated, Hierarchical System Protection

An example of the novel transmission system protection philosophy that relies on local and wide area protection methods is presented in this section. This approach allows automated system-wide monitoring of system component condition, reliable protective relay operation and performs corrective actions in the case protection dependability or security is compromised. The scope of the proposed approach includes:

- **Predictive Protection:** The system monitoring and control tool that performs routine vulnerability analysis of operating condition of the whole system and individual elements [24-26] is deployed at the control center level and alert signals are sent to the substation level to closely monitor relays placed at the most vulnerable components. The prediction of where the protection misoperation may occur gives an early warning of how the contingencies may unfold.

- **Inherently Adaptive Protection:** At the substation level neural network based fault detection and classification algorithm [27-32] is employed. Its tripping logic is based on feature patterns of waveform measurements that are recognized on line and matched to the patterns obtained during learning process that includes thousands of potential fault conditions. This approach does not have settings and hence avoids misoperation due to inadequate settings allowing for an inherent adaptive action to optimize the balance between dependability and security.
- **Corrective Protection:** At the substation level fast and accurate synchronized sampling based fault location [32-35] and event tree analysis [26,28] to detect incorrect line tripping sequence and incorrect relay logic operation respectively. Upon transmission line tripping, fault location algorithm will validate correctness of relay's operation and in case of unconfirmed fault condition, the system component (transmission line) will be quickly restored. The relay logic will be checked as it executes and if an incorrect sequence is detected, the relay action will be corrected.

The following sections give detail description of the components of the proposed approach and provide study case in which this methodology is used for analysis, as well as early detection and mitigation of cascading outages.

5.3.1. Predictive Protection

The proposed system monitoring and control tool utilizes wide area measurements to evaluate the vulnerability and security of the power system during dynamically changing conditions. For the routine static and dynamic contingency analysis, contingencies which can lead to an overload condition, voltage problem, angle instability, voltage instability, etc., will be found and taken care of. The vulnerability analysis for each system element, as well as for the whole system is utilized in routine contingency analysis. The operation of the relays assigned to vulnerable system components is closely monitored and verified by applications at substation level.

The system is vulnerable if contingencies lead to an interruption of service as a result of a cascade. The element is vulnerable if contingencies or changing conditions lead to violation of the element limit, outage or malfunction of the element. Before the power system faces interruption of service or the element faces outage or mal-function, some indices can be used to represent the degree of vulnerability and security. Vulnerability index (VI) and margin index (MI) are proposed to represent comprehensive and quantitative vulnerability and security assessment of the individual part and whole system. Given a system with m generators, n buses, p lines and q loads, we define VI and MI sets as follows:

1. Vulnerability Index and Margin Index for Generators

$$VI_{P_{g,i}} = \frac{W_{P_{g,i}}}{2N} \left(\frac{P_{g,i}}{P_{g,i,max}} \right)^{2N}$$

$$VI_{P_{Q_{g,i}}} = \frac{W_{Q_{g,i}}}{2N} \left(\frac{Q_{g,i}}{Q_{g,i,max}} \right)^{2N}$$

$$VI_{gen_{loss},i} = VI_{gen_{loss},i} k_{gen_{loss},i}$$

$$VI_{gen} = \sum_{i=1}^m (VI_{P_{g,i}} + VI_{P_{Q_{g,i}}} + VI_{gen_{loss},i})$$

$$MI_{P_{g,i}} = 1 - \left(\frac{P_{g,i}}{P_{g,i,max}} \right)$$

$$MI_{Q_{g,i}} = 1 - \left(\frac{Q_{g,i}}{Q_{g,i,max}} \right)$$

2. Vulnerability Index and Margin Index for Buses

$$VI_{V,i} = \frac{W_{V,i}}{2N} \left(\frac{V_i - V_i^{sche}}{\Delta V_{i,lim}} \right)^{2N}$$

$$VI_{Loadab,i} = \frac{W_{Loadab,i}}{2N} (r_{Loadab,i})^{2N}$$

$$VI_{load_{loss},i} = W_{load_{loss},i} k_{load_{loss},i}$$

$$VI_{bus} = \sum_{i=1}^n (VI_{V,i} + VI_{Loadab,i} + VI_{load_{loss},i})$$

$$MI_{V,i} = 1 - \left| \frac{V_i - V_i^{sche}}{\Delta V_{i,lim}} \right|$$

$$MI_{Loadab,i} = 1 - r_{Loadab,i}$$

3. Vulnerability Index and Margin Index for Branches

$$VI_{P_f,i} = \frac{W_{P_f,i}}{2N} \left(\frac{P_{f,i}}{S_{i,max}} \right)^{2N}$$

$$VI_{Q_f,i} = \frac{W_{Q_f,i}}{2N} \left(\frac{Q_{f,i}}{S_{i,max}} \right)^{2N}$$

$$VI_{Q_c,i} = \frac{W_{Q_c,i}}{2N} \left(\frac{Q_{c,i}}{Q_\epsilon} \right)^{2N}$$

$$VI_{Line_angle,i} = \frac{W_{Line_angle,i}}{2N} \left(\frac{La_i}{La_{i,max}} \right)^{2N}$$

$$VI_{Relay,i} = \frac{W_{Relay,i}}{2N} \left(\left(\frac{1}{d_{sr,i}} \right)^{2N} + \left(\frac{1}{d_{rs,i}} \right)^{2N} \right)$$

$$VI_{line_loss,i} = W_{line_loss,i} k_{line_loss,i}$$

$$VI_{line} = \sum_{i=1}^p (VI_{Pf,i} + VI_{Qf,i} + VI_{Qc,i} + VI_{Line_angle,i} + VI_{line_loss,i})$$

$$MI_{Sf,i} = 1 - \frac{Sf_i}{S_{i,max}}$$

$$MI_{line_angle,i} = 1 - \frac{Laf_i}{La_{i,max}}$$

$$MI_{Relay,i,sr} = d_{sr,i} - K_z \left| \sin\left(\frac{\pi}{2} - \alpha + \theta_{d,sr}\right) \right|$$

$$MI_{Relay,i,rs} = d_{rs,i} - K_z \left| \sin\left(\frac{\pi}{2} - \alpha + \theta_{d,rs}\right) \right|$$

Where:

VI_{xx} : vulnerability index for different parameters,

MI_{xx} : margin index for different parameters,

WI_{xx} : weighting factor for different parameters, based on the system operating practice. If the operators are more concerned with one part, they can assign larger weight to that part.

$k_{x_loss,i}$: loss ratio, between 0 and 1. 0: no loss; 1: complete loss;

N : 1 in general,

$r_{Loadab,i}$: bus loadability,

Pf_i, Qf_i, Sf_i : line real, reactive and apparent power,

Qc_i : individual line charging,

Q_{ϵ} : total reactive power output of all generators, or total reactive power of the whole system,

La_i : individual bus voltage angle difference at each line,

$La_{i,max}$: bus voltage angle difference limit at each line,

$d_{sr,i}, \theta_{d,sr}$: magnitude and angle of normalized apparent impedance seen by distance relay located at the sending end of that line and looking at the receiving end,

α : line impedance angle,

K_z : zone setting,

$MI_{Relay,i,sr}, MI_{Relay,i,rs}$: defined as the distance from the apparent impedance seen by transmission line distance relay to the relay protection zone circle; zero or negative values mean the apparent impedance is at or within the protection zone circle.

As shown above, the relay behavior needs to be monitored carefully from the system side. The competitive market operation causes changing operating conditions, where change of the generation pattern and change of the energy transfer between generator and load are frequent. This results in frequent changes of power flow patterns through the transmission network and significant changes of the bus voltages and line currents. During the normal operation condition, the behavior is still within the system security limit and there is no problem with the protective relay expected operation. However, after some outages, the system operating security might be degraded. Some transmission lines may have overload conditions and their connected buses may have low voltage problems. The apparent impedance seen by distance relays may fall into their backup protection zones. They may trip the healthy lines if the lasting time is longer than the setting time period and may further trigger a cascading outage. Voltages and currents obtained from the power flow method or system-wide phasor measurements are used to calculate the apparent impedance seen by distance relay:

$$z_{d,ij} = \frac{V_i}{I_{ij}} = \frac{V_i}{(V_i - V_j)/z_{ij}}$$

$$z_{d,ij} = \frac{z_{d,ij}}{z_{ij}} = \frac{V_i}{(V_i - V_j)} = \frac{|V_i|}{|V_i - V_j|} \angle \theta_{d,ij} = d_{ij} \angle \theta_{d,ij}$$

$$D_{i,j} = d_{i,j} - K_z \left| \sin\left(\frac{\pi}{2} - \alpha + \theta_{d,ij}\right) \right|$$

Where:

V_x : voltage of buses i and j ,

I_x : line current from bus i to bus j ,

z_{ij} : impedance of line i, j ,

$z_{d,ij}$: apparent impedance seen by distance relay from bus i to bus j of line i, j ,

$\underline{z}_{d,ij}$: normalized apparent impedance seen by distance relay from bus i to bus j ,

$d_{i,j}, \theta_{d,ij}$: magnitude and angle of normalized apparent impedance $\underline{z}_{d,ij}$,

α : line i, j impedance angle,

K_z : zone setting,

$D_{i,j}$: defined as the distance from the apparent impedance seen by transmission line distance relay to the relay protection zone circle, zero or negative values mean the apparent impedance is at or within the protection zone circle.

For the line distance relay (with *mho* characteristic), it will operate if

$$|z_{d,ij} - \rho| \leq |\rho|$$

Where:

$$\rho = \beta_{z_{ij}}/2$$

Normalize as:

$$|z_{d,ij} - \beta/2| \leq \beta/2$$

For typical relay settings, for zone 1, choose $\beta = 0.8$; for zone 2, choose $\beta = 1.2$. Zone 3 relay settings are power system dependent, here we can simply choose 2.4 or choose settings to protect the full length of next longest neighboring line.

During the system normal operation or dynamic changing conditions, normalized apparent impedance and distance relay margin can be calculated for the monitoring of distance relay performance. If the apparent impedance is close to relay protection zone, warning information will be given and careful monitoring of the associated distance relay is required by the substation module.

5.3.2. Inherently Adaptive Protection

The traditional transmission line protection schemes are mostly based on calculation of features of certain electric signals and their comparison to predefined thresholds often called “settings”. This kind of method relies on a “hard” criterion. The settings require complex system analysis to cover worst case fault conditions. This method can only consider one fault scenario at a time; hence the flexibility is limited. The threshold based algorithm needs extensive theoretical analysis and final verification comes from field performance evaluations, which may be ineffective if a major deficiency is discovered through blackouts. The above issues can be avoided by applying a “soft” criterion based on artificial intelligence techniques. The neural network is such a technique and has been studied in the power system area for quite a while [30, 31]. Its major advantage is that it can take into account several features of the input signals simultaneously and compare the patterns according to their mutual similarity instead of the “hard” thresholds.

The block diagram of fuzzy ART neural network algorithm used for fault diagnosis is demonstrated in Figure 20. The two major components of the algorithm are neural network training and fuzzy K-NN classification. The theoretical background of these two approaches can be found in [66]. By using those techniques, the fault detection and classification becomes a pattern recognition approach instead of phasor computation and comparison against setting. Without calculating the impedance phasor, the voltage and current signals from the local measurement are formed as patterns using time domain data samples, which can retain the original information in the waveforms. Without need to specify settings, the setting coordination task and associated inaccuracies can be avoided. Thousands of patterns obtained from power system simulation or substation database of field recordings are used to train the neural network offline and then the pattern prototypes are used to detect the real faults online by using the fuzzy K-nearest neighbor (K-

NN) classifier. A graphic view of the status of input patterns at each step during training and testing process is shown in Figure 21.

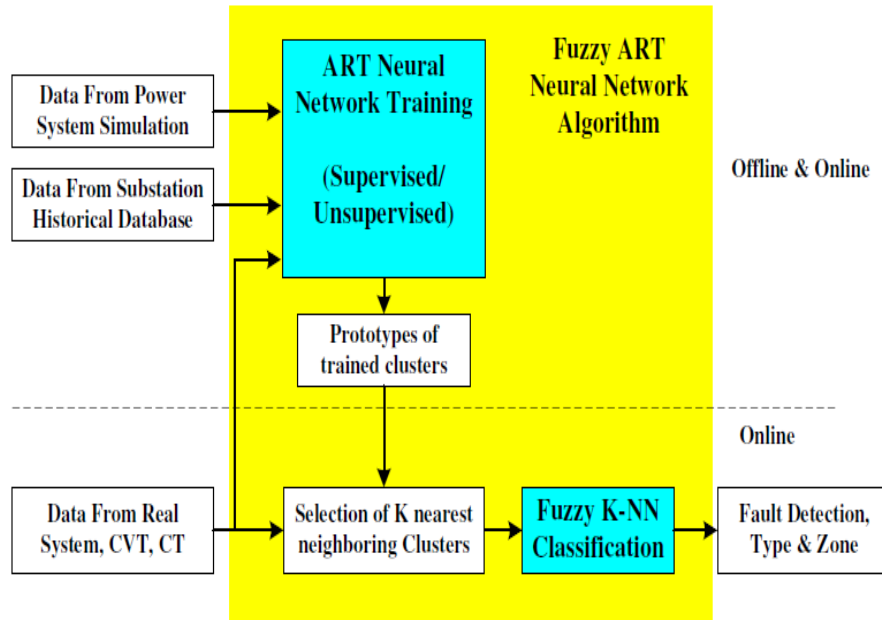


Figure 20: Fuzzy ART Neural Network Training Process for Fault Diagnosis Algorithm

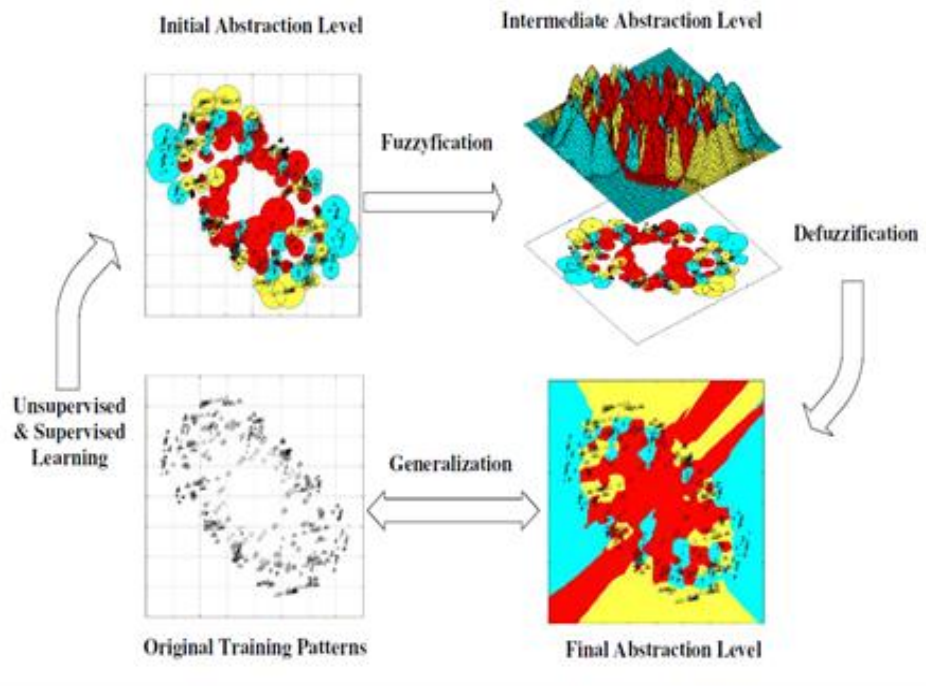


Figure 21: Formation of Patterns During Training and Testing

The objective of neural-network training is to allocate the input data into several prototype clusters that belong to same categories or classes according to their mutual similarity. The neural-network training uses a mechanism of clustering technique with combined unsupervised and supervised learning. The architecture is shown in Figure 22.

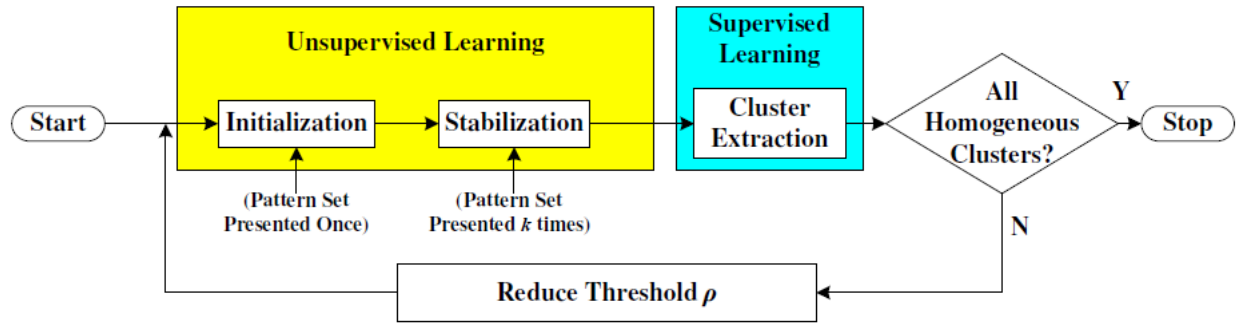


Figure 22: Architecture of Neural Network Training

Unsupervised learning consists of two steps: initialization and stabilization. In an initialization phase, the entire pattern set is presented only once to establish initial cluster structure based on similarity between patterns. The Euclidean distances between patterns are measured and compared to the current threshold (radius of the cluster) to decide whether they belong to same clusters. In stabilization phase, the entire pattern set is being presented to the NN numerous times and the process is similar to that in initialization phase. The iterations will not end until the initial unstable cluster structure becomes stable and no patterns change clusters after a single iteration.

During supervised learning, the class label is assigned to each input pattern allowing separation of homogenous (all patterns belong to same class) and nonhomogeneous clusters produced in unsupervised learning. For homogeneous clusters, their position, size, and category are stored into the memory and the patterns from those clusters are removed from current training pattern set. The remaining patterns, presented in nonhomogeneous clusters, are left for new learning iterations. When all clusters are examined, the new data set is sent to next unsupervised/supervised learning iteration with reduced threshold. The entire learning process is completed when all the patterns are grouped into homogeneous clusters with predefined class labels.

The advantage of this kind of neural network is that the number of clusters is increased and their positions are updated automatically during the learning, and there is no need to define them in advance. This is the reason why the selection of the number of hidden neurons is not an issue in this method. Regarding large data set and convergence issue, the data set can be separable no matter how many input data are presented since the size of the clusters can be reduced infinitely during training. The prototypes of trained clusters are used for online detection of unknown patterns. If the new pattern falls in the sphere of a cluster, the pattern is assigned to the category that cluster belongs to. If the new pattern falls in an unclaimed area, fuzzy-nearest neighbor (-NN) algorithm [66] is used for assigning its category by taking into account the influence of surrounding clusters.

5.3.3. Corrective Protection

Fault location is a very useful tool to accurately locate the fault and verify the occurrence of the fault. The fault location can confirm whether a fault has indeed occurred on the line. If computed on-line, it can also serve as a relay verification tool for a back-up fault confirmation. When the fault is precisely located, one should know which breakers are responsible to clear that fault, and unnecessary trips that could spread an outage could be avoided. Both the dependability and security of protection system operation will be improved by incorporating a precise fault location function.

Synchronized sampling based fault location algorithm uses raw samples of voltage and current waveforms synchronously taken from two ends of the transmission line [63-65]. This can be achieved using Global Positioning Satellite (GPS) receivers, which generate the clock time reference for data acquisition equipment. It has two types of applications dealing with the short line lumped model and long line distributed model, which is shown in Figure 23.

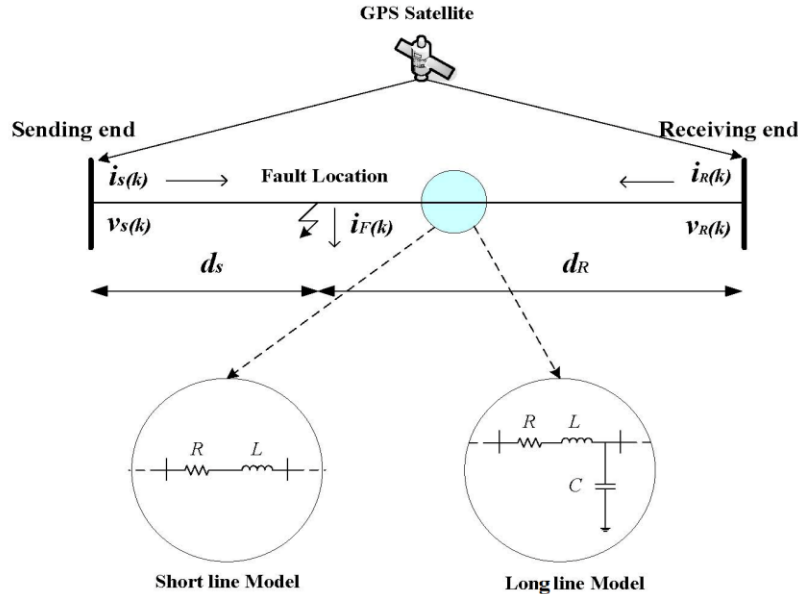


Figure 23: Synchronized Sampling Based Fault Location

The algorithm is derived by solving the transmission line differential equations. Short line algorithm and long line algorithm are derived using lumped RL line parameters and distributed RLC line parameters respectively. The operation of this algorithm is demonstrated with the transmission line shown in Figure 24. The voltage and current at the faulted point can be represented by both sending end data and receiving end equations using linear relationship because the homogenous-parameter line is separated by the fault point. If there is no fault on the line, the fault location cannot be found because there are multiple solutions in that case. Different algorithms use different techniques to find the fault point [63, 65].

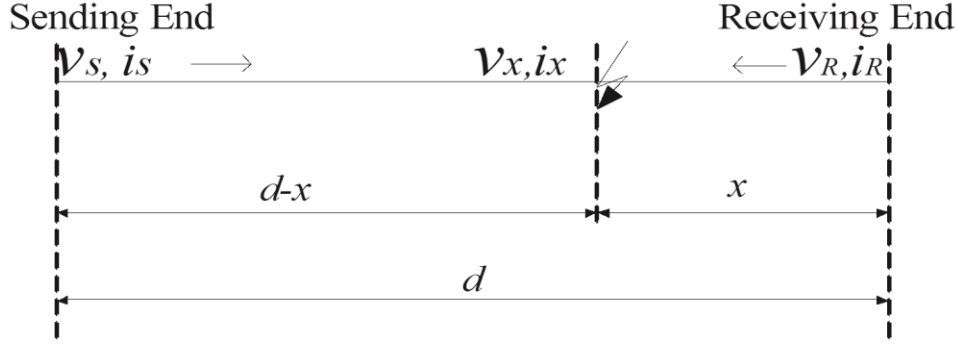


Figure 24: A Faulted Transmission Line

Short Line Model: For short line, which is usually shorter than 50 miles, the fault location can be calculated directly using minimum square estimate method, as follows [65]:

$$x = \frac{- \sum_{m=a,b,c} \sum_{k=1}^N \hat{a}_m A_m(k) B_m(k)}{\sum_{m=a,b,c} \sum_{k=1}^N \hat{a}_m B_m^2(k)}$$

Where:

$$A_m(k) = v_{mS}(k) - v_{mR}(k) - d \sum_{p=a,b,c} \left[\left(r_{mp} + \frac{l_{mp}}{Dt} \right) i_{pS}(k) - \frac{l_{mp}}{Dt} i_{pS}(k-1) \right] \quad m = a, b, c$$

$$B_m(k) = \sum_{p=a,b,c} \left\{ \left(r_{mp} + \frac{l_{mp}}{Dt} \right) [i_{pS}(k) + i_{pR}(k)] - \frac{l_{mp}}{Dt} [i_{pS}(k-1) + i_{pR}(k-1)] \right\} \quad m = a, b, c$$

Where k is the sample point, Dt is sampling period, subscripts S, R stand for the values from sending end and receiving end of the line.

Long Line Model: For long transmission line model, we can only build the voltage and current profiles along the line using revised Bergeron's equation [68]:

$$v_{j,k} = \frac{1}{2} [v_{j-1,k-1} + v_{j-1,k+1}] + \frac{Z_c}{2} [i_{j-1,k-1} + i_{j-1,k+1}] - \frac{RLx}{4} [i_{j-1,k-1} + i_{j-1,k+1}] - \frac{RDx}{2} i_{j,k}$$

$$i_{j,k} = \frac{1}{2Z_c} [v_{j-1,k-1} - v_{j-1,k+1}] + \frac{1}{2} [i_{j-1,k-1} + i_{j-1,k+1}] + \frac{RLx}{4Z_c} [i_{j-1,k+1} - i_{j-1,k-1}]$$

Where $Dx = Dt / \sqrt{lc}$ is the distance that the wave travels with a sampling period Dt ; $Z_c = \sqrt{l/c}$ is the surge impedance. Subscript "j" is the position of the discretized point of the line and "k" is the sample point.

The final location on long transmission lines is obtained by an indirect method, as shown in Figure 25.

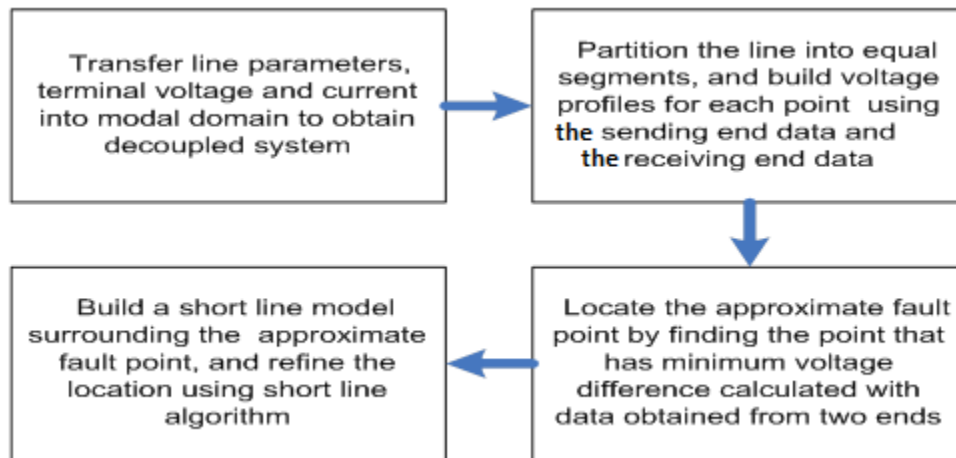


Figure 25: Steps for Long Line Fault Location Algorithm

The accuracy of both algorithms is dependent on accuracy of data sampling synchronization, sampling rate and correctness of line model parameters.

Event tree analysis is a commonly used event/response technique in industry for identifying the consequences that can result following an occurrence of an initial event [67]. We can use it as an on-line monitoring tool for relay operations to indicate what happens as a consequence of a disturbance and what activities are taken by relays or other control methods. This information can also contribute to corrective relaying action if it is determined that the anticipated relaying action has not unfolded as expected.

An example of event tree analysis is shown in Figure 26. The node stands for the status after an event happened or an action is taken. The white ones represent correct actions and the black ones represent incorrect actions. Table 21 gives the explanation of the meaning of each node. The whole event tree should cover all possible activities following the root node (initial event). Finally, the actual event evolution path is monitored to see if the activities are approaching a final expected status. If not, a corrective action needs to be issued. For a single distance relay, at least three event trees need to be built to match three types of initial events: (1) No fault detected in either primary zone or backup zones; (2) Fault detected in the primary zone; (3) Fault detected in backup zones. A design of the three kinds of event trees can be found in [62].

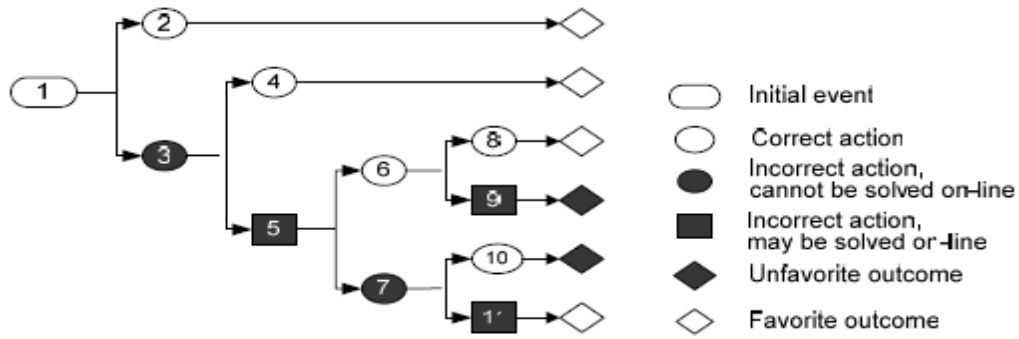


Figure 26: No Fault Condition

Table 21: Scenarios and Reference Actions for the Nodes of Event Tree

<i>Node</i>	<i>Scenarios</i>	<i>Reference Action</i>
1	No fault in preset zones	Keep monitoring
2	Relay does not detect a fault	Stand by
3	Relay detects a fault	Check the defects in relay algorithm and settings
4	Trip signal is blocked	
5	Trip signal is not blocked	Send block Signal if necessary
6	Circuit breaker opened by the trip signal	
7	Circuit breaker fails to open	Check the breaker circuit.
8	Autoreclosing succeeds to restore the line	
9	Autoreclosing fails to restore the line	Send reclosing signal to the breaker
10	Breaker failure protection trips all the breakers at the substation	
11	No Breaker failure protection or it doesn't work	Check the circuit of the breaker failure protection.

When a suspect disturbance is detected, either by relay or by the fault analysis tool, the local analysis tool will find the matching event tree according to the fault analysis result. Then the actual relay operations will be tracked in that event tree and finally the event sequence of that relay system will be obtained. This information will be sent to the system analysis tool for further system security analysis. The misoperations of relays can be corrected by local action quickly or mitigated by system security control after a detailed system-wide analysis.

As a summary, the three concepts proposed earlier are tied together in an overall solution design shown in Figure 27.

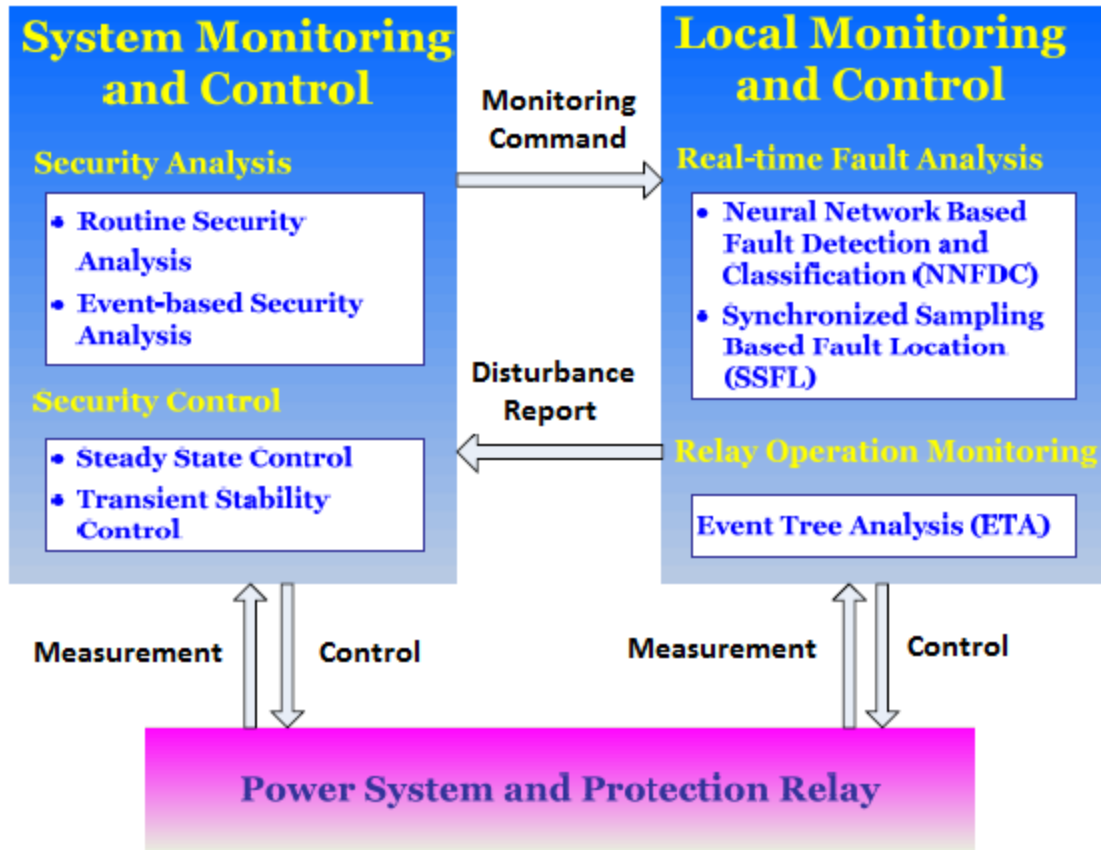


Figure 27: The Hierarchical System Protection Architecture

The system-wide event-based analysis will get the disturbance information from system measurements and local analysis. If such events are studied by the routine security analysis, pre-determined emergency control means will be activated. If the events are unexpected, transient stability analysis and power flow analysis will be run to see whether there are transient stability or steady state problems. If so, associated control means will be found and issued to mitigate such events.

5.3.4. Study Case

In order to illustrate the use and operational efficiency of the proposed Coordinated, Hierarchical System Protection scheme, the IEEE 39-bus New England test system shown in Figure 23 is utilized. The two most vulnerable lines according to their vulnerable indices are: Line 21-22,28-29. The outage of those lines will have a large impact for the system stability since the original loads in those two lines will be re-distributed to the neighboring lines causing more overloading issues. The system monitoring tool will inform the local relay monitoring tool on those lines to monitor the relay operations closely.

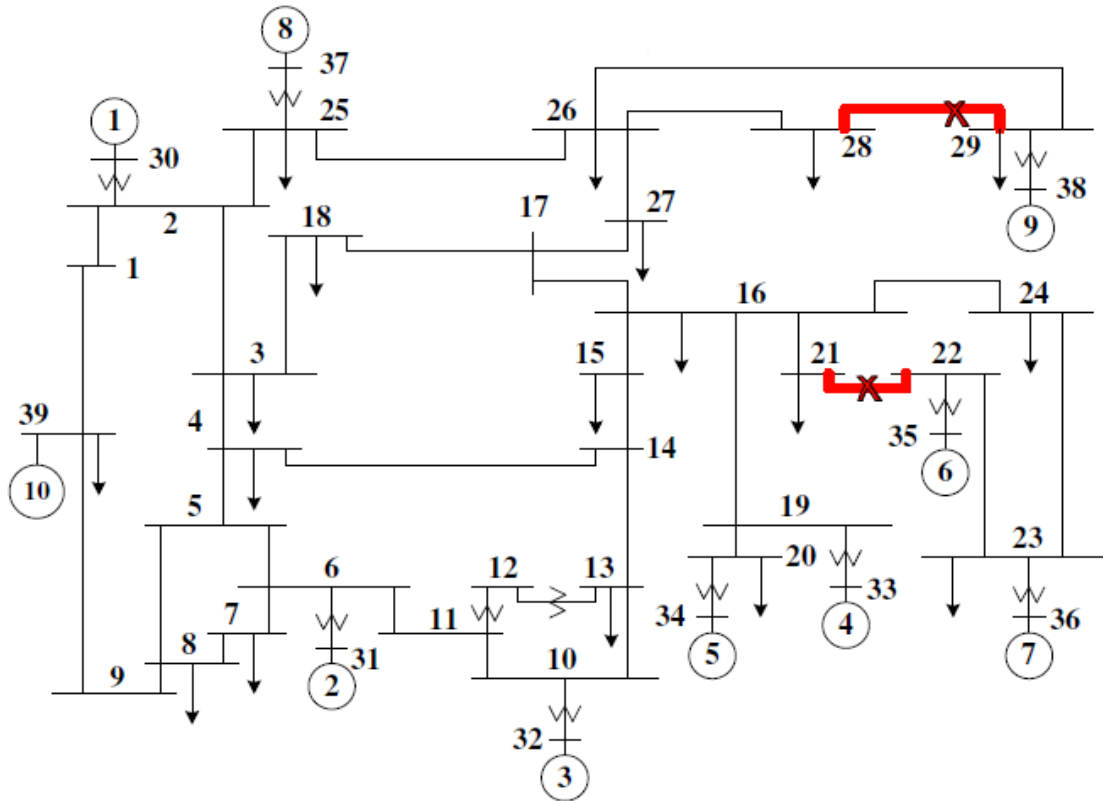


Figure 28: IEEE 39-Bus System

Assume a series of disturbances occur in the system, on system components are marked in Figure 28; description of the event sequence follows in Figure 29. These two faults are permanent faults and thus isolated by the relay actions. After the line 21-22 are removed due to the first fault, the top 2 most vulnerable lines are changed to: Line 28-29, 2-3. After the line 28-29 are removed due to the second fault, the top 2 most vulnerable lines are changed to: Line 23-24, 26-29. This contingency may cause relay at Bus 26 of Line 26-29 to misoperate. The trajectory of impedance seen by that relay is shown in Figure 30 with the event sequence labeled. Although the two faults are not related to the healthy line 26-29, the power swing caused by the two faults will have an impact on the distance relay. It observes Zone 3 fault at 1.627s after the second fault clearing until the trajectory leaves Zone 3 circle at 1.998s. The distance relay may trip Line 26-29 when its Zone 3 timer expires. As a result, buses 29, 38 will be isolated from the system, including the G9 and loads at bus 29. This will result in the oscillation in the rest of the system and further cascading outage may happen.

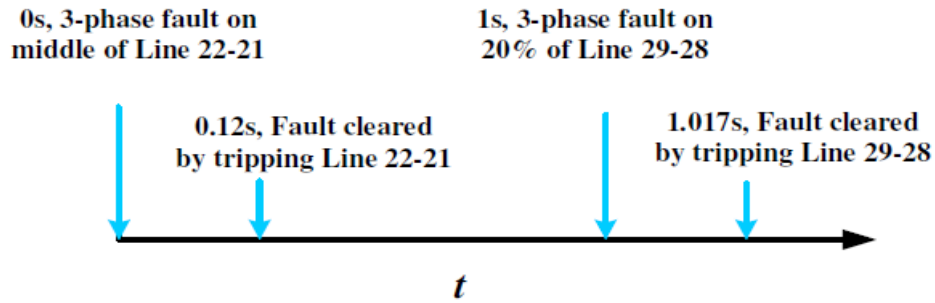


Figure 29: Event Sequence

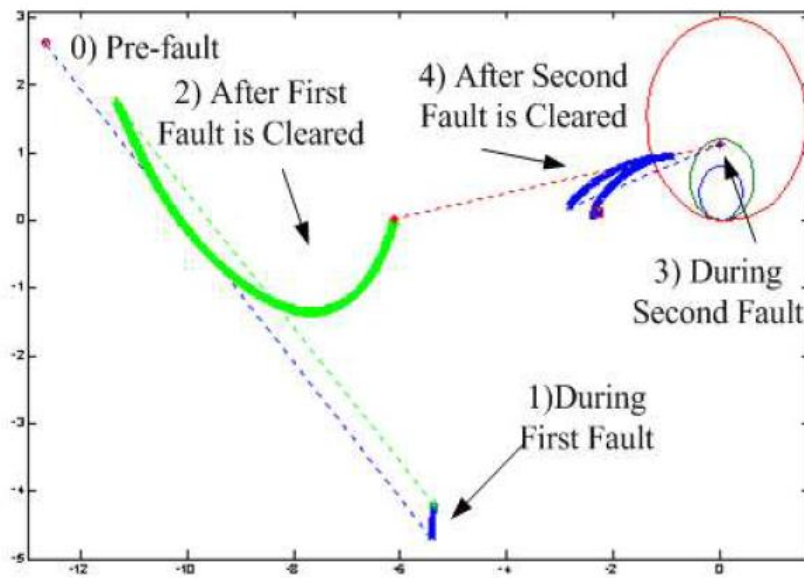


Figure 30: Trajectory of Impedance

The mentioned situation can be prevented by the proposed system and local monitoring and protection tool. When the first fault occurs, the faulted line 21-22 is removed and no other operation happens. The relay monitoring tool for the relay at Line 21-22 will inform the system monitoring tool about the relay operation for the three-phase fault. The system security analysis is activated after the first fault. An alert signal will be sent to the local relay monitoring tool at vulnerable lines at this stage. Since the first fault will not degrade the system stability very much, the local relay monitoring tool will not be authorized to intervene with relay operations at this stage. When the second fault happens and Line 28-29 is removed, the local relay monitoring tools for the most vulnerable lines 23-24 and 26-29 will be authorized to correct the potential relay misoperation or unintended operation in real time since the misoperation of those relays will directly separate the system. After the second fault, the local relay monitoring tool at Line 26-29 will draw a conclusion to block the relay from tripping for Zone 3 fault. That information will be sent back to the system. The system will issue appropriate control means to mitigate the disturb-

ances. In an actual large scale system, it is impossible that one or two contingencies like the ones discussed in this scenario can cause large scale system oscillation. Usually there is enough time for coordinating the system-wide and local analysis in the initial stages of the disturbances to mitigate the impact of the disturbances before they unfold into the large one. An interactive system-wide and local monitoring and control means can really help reduce the probability of a cascading blackout since the disturbances can be fully analyzed at both the local and system level.

5.3.5. Future Work

In this section several protection problems in distribution systems with high DG penetration are described. The objective is to investigate those problems further in the next project stage and to recommend solutions using proposed Coordinated, Hierarchical System Protection framework.

In the traditional distribution system protection schemes are designed based on the assumptions that there is only power flow in a single direction and that fault current has much higher magnitude than normal current and that it decays downstream with the distance from the fault. However, those assumptions may not validate in the systems with high DG penetration. The power can flow upstream of the feeder affecting the coordination and operation of the standard overcurrent protection schemes. Protection under-reach, sympathetic trips, unsuccessful clearing of faults, and unintentional islanding are all major problems associated with the utilization of DG systems in the distribution systems.

Protection under-reach refers to the potential misoperation of a relay during fault conditions due to the decrease in fault current. Referring to Figure 31, in the absence of DG, a fault at the specified location would be fed entirely by the grid, resulting in a large current magnitude being detected by the relay at CB2. However, when a DG unit is present, a portion of the fault current is provided by the DG unit, which might be negligible.

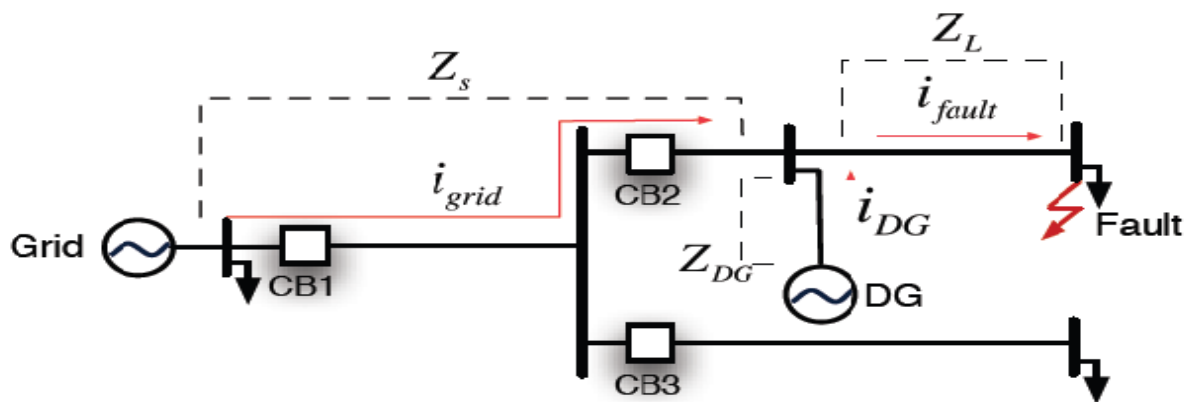


Figure 31: Overcurrent Under-Reach [69]

The Thévenin equivalents for the cases with and without DG are shown in Figure 32. It can be seen that the grid current contribution is less when DG is present. The current seen

by the relay at CB2 is consequently less, potentially preventing the fault from being detected.

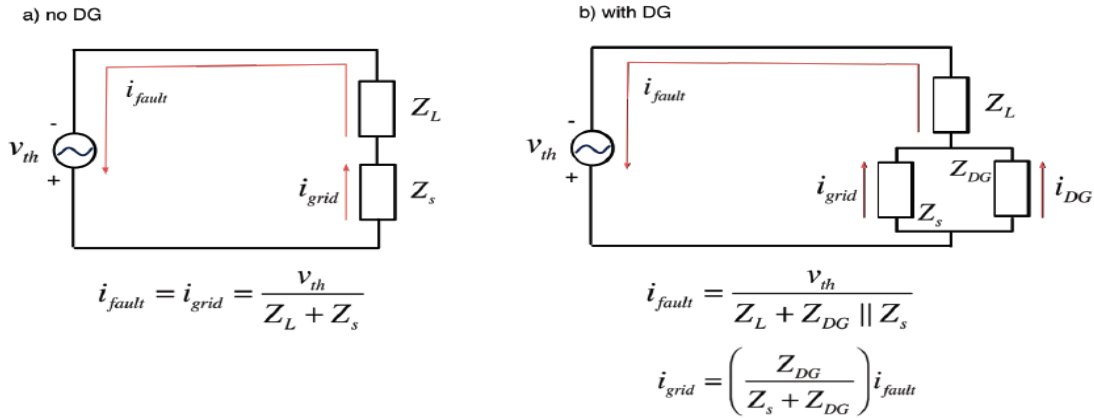


Figure 32: Thevenin Equivalent of the System with and without DG [69]

Sympathetic trip involves the isolation of a healthy feeder in the event of a fault on a neighboring feeder due to reverse power flow from DG units. Referring to Figure 33, in the absence of DG, a fault at the specified location would be detected by the relay at CB3. However, when a DG unit is present, the current from DG would also feed the fault. If the DG fault current is large enough, the relay at CB2 may also trip, unnecessarily isolating the healthy feeder.

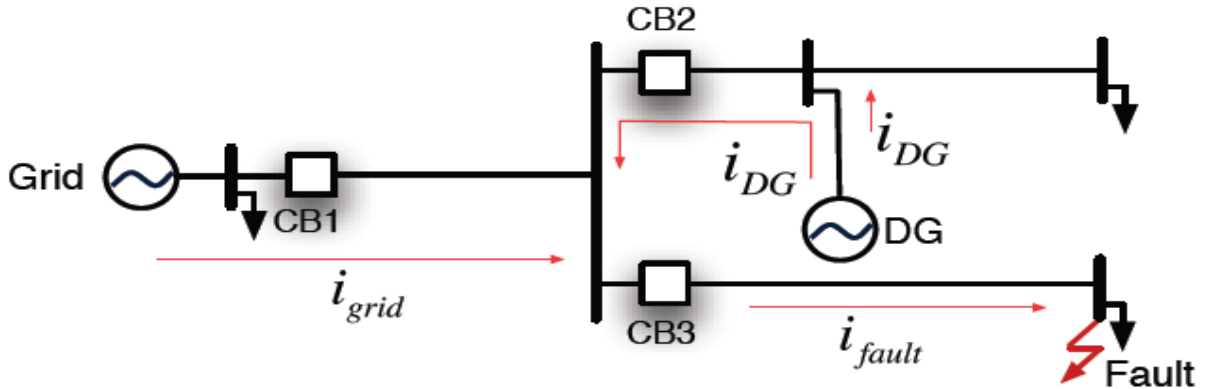


Figure 33: Overcurrent Sympathetic Trip [69]

Unintentional islands are formed when the grid is disconnected by the protection scheme, but the DG units are still active and can continue to feed faults. Since current is still flowing, automatic reclosure fails as the continued presence of the fault current would force the grid to trip out again. In addition to unsuccessful reclosing, possible frequency variation in the DG units can cause the grid-side and island-side systems to slip out of phase. If no synchronization function is present, reclosure can occur when the phase difference between the two ends is significant. This would result in large current and voltage transi-

ents and potentially damage the DG units or feeder components. Moreover, in the event of unintentional islanding, and active portions of the system can become safety hazards for personnel.

6. Conclusions

The trend in power system planning that utilizes tight operating margins with less redundancy, addition of distributed generators, and independent power producers, makes the power system more complex to operate and more vulnerable to disturbances. Current control strategies are sometimes inadequate to stop the spreading of disturbances. And in such cases, one could only rely on protective relays to protect the system from the widespread effects of fast disturbances. In this study we proposed new robust and reliable hierarchically coordinated protection approach that may be used in high voltage systems with high DG penetration. The benefits of the proposed approach are many. Through the analysis result from the system-wide centralized tool, the local side can know whether its relay system needs to be monitored closely or not. Through the analysis result from the local protection tool, the system side can understand exactly the disturbance information in real time and take fast and accurate control actions.

The proposed framework may be used in defining new protection scheme for distribution system too. It is well known that existing protection practice with overcurrent relays in cases with high DG penetration are ineffective due to problems in finding right settings and problems in relay coordination. There is need for more reliable, robust and accurate protection scheme. In the new protection approach for distribution system, lightning location data may be used as a part of prediction protection module, adaptive overcurrent protection featured with advanced machine learning and pattern recognition technique may be used as a part of adaptive protection module and fast fault location [70] as a part of corrective protection module.

References

- [1] Kansal, P.; and A. Bose. *Smart Grid Communication Requirements for the High Voltage Power System*. IEEE PES General Meeting, pgs. 1-6, July 2011.
- [2] Tholomier, D.; H. Kang, and B. Cvorovic. *Phasor Measurement Units: Functionality and Applications*. IEEE PES Power Systems Conference & Exhibition, pgs. 1-12, March 2009.
- [3] Wu, F. F.; K. Moslehi, and A. Bose. *Power system control centers, past, present and future*. Proceedings IEEE, vol. 93, no. 11, pgs. 1890–1908, November 2005.
- [4] Martin, K.; and J. Carroll. *Phasing in the technology*. Power and Energy magazine, IEEE, vol. 6, no. 5, pgs. 24–33, September-October 2008.
- [5] Thorp, J. S.; A. Abur, M. Begnovic, J. Giri, and R Avila-Rosales. *Gaining a wider perspective*. Power and Energy magazine, IEEE, vol. 6, no. 5, pgs. 43-51, September-October 2008.
- [6] Phadke, A.; and J.S. Thorp. *Synchronized Phasor Measurements and Their Applications*. Springer, January 2008.
- [7] Marinez, C.; M. Parashar, J. Dyer, and J. Coroas. *Phasor Data Requirements for Real Time Wide-Area Monitoring, Control and Protection Applications*. CERTS/EPG, EIPP-Real Time Task Team, January 2005.
- [8] *Phasor measurement application study*. California Institute for Energy and Environment, October 2006.
- [9] Carson, C. W.; D. C. Erickson, K. E. Martin, R. E. Wilson, and V. Venkatasubramanian. *WACS-Wide-area stability and voltage control systems: R&D and online demonstration*. Proceedings IEEE, vol. 93, no. 5, pgs. 892–906, May 2005.
- [10] Tomsovic, K.; D. E. Bakken, V. Venkatasubramanian, and A. Bose. *Designing the next generation of real-time control, communications and computations for large power systems*. Proceeding IEEE, vol. 93, no. 5, pgs. 965–979, May 2005.
- [11] *Actual and potential Phasor data applications*. NASPI, July 2009. Available at: <http://www.naspi.org/phasorappstable.pdf>
- [12] *Phasor Application Classification*. NASPI Data and Network Management Task Team, August 2007. Available at: http://www.naspi.org/resources/dnmtt/phasorapplicationclassification_20080807.xls
- [13] Bose, A. *Smart Transmission Grid Application and Their supporting Infrastructure*. IEEE Transactions on Smart Grid, vol. 1, no. 1, pgs. 11-19, June 2010.
- [14] Yang, T.; H. Sun, and A. Bose. *Two level PMU based Linear State Estimator*. pgs. 1-6, IEEE PES Power Systems Conference & Exhibition, March 2009.
- [15] Gjermundrod, H.; D. E. Bakken, C H Hauser, and A. Bose. *GridStat: A Flexible QoS-Managed Data Dissemination Framework for the Power Grid*. IEEE Transactions on Power Delivery, vol. 24, no. 1, pgs. 136-143, January 2009.

- [16] Hauser, C.; D. Bakken, and A. Bose. *A failure to communicate: Next generation communication requirements, technologies, and architecture for the electric power grid*. Power and Energy Magazine, IEEE, vol. 3, no. 2, pgs. 47–55, March-April 2005.
- [17] IEEE standard for Synchrophasors for Power Systems, IEEE Std. C37.118- 2005.
- [18] Chenine, M.; K. Zun, and L Nordstrom. *Survey on priorities and communication requirements for PMU-based applications in the Nordic Region*. IEEE Power Tech, pgs. 1-8, July 2009.
- [19] *Case data provided with MATPOWER-4.0*. Available at: <http://www.pserc.cornell.edu/matpower/>.
- [20] *Ns manual*. Available at: http://www.isi.edu/nsnam/ns/doc/ns_doc.pdf.
- [21] *Ns2 Simulator for beginners*. Available at: <http://www-sop.inria.fr/members/Eitan.Altman/COURS-NS/n3.pdf>.
- [22] Hasan, R.; R. Bobba, and H. Khurana. *Analyzing NASPInet Data Flows*. IEEE PES Power Systems Conference & Exhibition, pgs. 1-6, March 2009.
- [23] Armenia, A.; and J.H. Chow. *A Flexible Phasor Data Concentrator Design Leveraging Existing Software Technologies*. IEEE Transactions on Smart Grid, vol. 1, no. 1, pgs. 73-81, June 2010.
- [24] Johnston, R. A.; et al. *Distributing Time-synchronous Phasor Measurement Data Using the GridStat Communication Infrastructure*. Hawaii International Conference on System Sciences, January 2006.
- [25] Muthuswamy, S. *System implementation of a real-time, content based application router for a managed publish-subscribe system*. Master’s thesis, Washington State University, 2008.
- [26] Anderson, P. M.; and A. A. Fouad. *Power system control and stability*. Iowa State University Press, p. 450, 1977.
- [27] Kansal, P. *Communication requirements for smart grid applications for power transmission systems*. Master’s thesis, Washington State University, 2011.
- [28] *MATLAB file used after modification*. Available at: <http://www.mathworks.com/matlabcentral/fileexchange/13457-kruskal-algorithm>.
- [29] Korab, R. *Locational marginal prices (and rates) – Harmonization of markets solutions with new development trends*. Acta Energetica, no 2, pgs. 31-40, 2009.
- [30] Eto, J. H.; et al. *Use of Frequency Response Metrics to Assess the Planning and Operating Requirements for Reliable Integration of Variable Renewable Generation*. Lawrence Berkeley National Laboratory, LBNL-4142-E, December 2010.
- [31] Wellinghoff, J.; D. L. Morenoff, J. Pederson, and M.E. Tighe. *Creating Regulatory Structures for Robust Demand Response Participation in Organized Wholesale Electric Markets Federal Energy Regulatory Commission*. Available at: [http://www.ferc.gov/about/com-mem/wellinghoff/ACEEE article.pdf](http://www.ferc.gov/about/com-mem/wellinghoff/ACEEE%20article.pdf) 2009.

- [32] ISO New England. *Alternative Technology Regulation Pilot Program Frequently Asked Questions*. Available at: <http://www.iso-ne.com/support/faq/atr/index.html>.
- [33] Saberi, A.; P. Sannuti and A. Stoorvogel. *Control of Linear Systems with Regulation and Input Constraints*. Springer-Verlag, London, UK, 2000.
- [34] LaMonica, M. *Grid storage gets updraft from auto batteries*. CNET News Service, September 7, 2010. Available at: http://news.cnet.com/8301-11128_3-20016711-54.html.
- [35] Baone, C. A.; and C. L. DeMarco. *Observer-based distributed control design to coordinate wind generation and energy storage*. Proceedings of the IEEE Power and Energy Society Conference on Innovative Smart Grid Technologies Europe, Gothenburg, Sweden, October 2010.
- [36] DeMarco, C. L.; and C. A. Baone. *Smart grid control design methods for distributed energy storage in frequency regulation markets*. Proceedings of the 18th IFAC World Congress, Milan, Italy, September 2011.
- [37] Baone, C. A.; and C. L. DeMarco. *From Each According to its Ability: Distributed Grid Regulation With Bandwidth and Saturation Limits in Wind Generation and Battery Storage*. to appear, IEEE Transactions on Control Systems Technology. Available at: http://ieeexplore.ieee.org/xpls/abs_all.jsp?arnumber=6142123&tag=1.
- [38] Baone, C. A.; and C. L. DeMarco. *Distributed Control Design to Regulate Grid Frequency and Reduce Drivetrain Stress in Wind Systems Using Battery Storage*. to appear, Proceedings of the 2012 American Control Conference, Montreal, Canada, June 2012.
- [39] Bergen, A. R.; and V. Vittal. *Power Systems Analysis*. Prentice Hall, Upper Saddle River, New Jersey, USA, 2000.
- [40] Bergen, A. R.; and D. J. Hill. *A structure preserving model for power system stability analysis*. IEEE Transactions on Power Apparatus and Systems, vol. PAS-100, no. 1, pp. 25 - 35, January 1981.
- [41] Johnson, V. H.; A. A. Pesaran, and T. Sack. *Temperature-dependent battery models for high-power Lithium-Ion batteries*. Presented at the 17th Electric Vehicle Symposium, Montreal, Canada, October 2000.
- [42] Ibraheem, P. Kumar; and D.P. Kothari. *Recent Philosophies of Automatic Generation Control Strategies in Power Systems*. IEEE Transactions on Power Systems, vol. 20, no. 1, ps. 346-357, February 2005.
- [43] Barton, J.P.; and D.G. Infield. *Energy storage and its use with intermittent renewable energy*. IEEE Transactions on Energy Conversion, vol. 19, no. 2, pgs. 441-448, June 2004.
- [44] Paatero, J.V.; and P. D. Lund. *Effect of energy storage on variations in wind power*. Wind Energy, vol. 8, no. 4, pgs. 421-441, March 2005.

- [45] Zhou, F.; G. Joos, C. Abbey, L. Jiao and B. T. Ooi. *Use of large capacity SMES to improve the power quality and stability of wind farms*. Proceedings of the 2004 IEEE Power Engineering Society General Meeting, June 2004.
- [46] Takahashi, R.; L. Wu, T. Murata and J. Tamura. *An Application of Flywheel Energy Storage System for Wind Energy Conversion*. Proceedings of the 2005 International Conference on Power Electronics and Drives Systems, 2005.
- [47] Dechanupaprittha, S.; K. Hongesombut, M. Watanabe, Y. Mitani and I. Ngamrool, *Stabilization of tie-line power flow by robust SMES controller for interconnected power system with wind farms*. IEEE Transactions on Applied Superconductivity, vol. 17, no. 2, pgs. 441 - 448, June 2007.
- [48] *Generic Type-3 Wind Turbine-Generator Model for Grid Studies*, WECC Wind Generator Modeling Group, Version 1.1, September 2006.
- [49] Undrill, J. *Power and frequency control as it relates to wind-powered generation*. Lawrence Berkeley National Laboratory report LBNL - 4143E, FERC/DOE contract no. DE-AC02-05CH11231, December 2010.
- [50] Lalor, G.; A. Mullane, and M. O'Malley. *Frequency control and wind turbine technologies*. IEEE Transactions on Power Systems, vol. 20, no. 4, pp. 1905 - 1913, Nov. 2005.
- [51] Duval, J.; and B. Meyer. *Frequency behavior of grid with high penetration rate of wind generation*. Proceedings of the 2009 IEEE Bucharest PowerTech, July 2009.
- [52] Chowdhury, B.H.; and H. T. Ma. *Frequency regulation with wind power plants*. Proceedings of the 2008 IEEE Power and Energy Society General Meeting - Conversion and Delivery of Electrical Energy in the 21st Century, July 2008.
- [53] De Almeida, R.J.; and J. A. P. Lopes. *Participation of doubly fed induction wind generators in system frequency regulation*. IEEE Transactions on Power Systems, vol. 22, no. 3, pgs. 944-950, August 2007.
- [54] Pai, M.A.; P.W. Sauer, and F. Dobraca. *A new approach to transient stability evaluation in power systems*. Decision and Control, 1988, Proceedings of the 27th IEEE Conference on , vol., no., pgs.676-680, vol.1, December 7-9, 1988.
- [55] Song, H.; and M.Kezunovic. *Static Security Analysis based on Vulnerability Index (VI) and Network Contribution Factor (NCF) Method*. IEEE PES Asia-Pacific Transmission & Distribution Conference & Exposition, China, August 2005.
- [56] Diss.Song, H. *The Detection, Prevention and Mitigation of Cascading Outages in the Power System*. Texas A&M University, 3296542, 2006.
- [57] Zhang, N.; and M. Kezunovic. *A Real Time Fault Analysis Tool for Monitoring Operation of Transmission Line Protective Relay*. Electric Power Systems Research Journal, vol. 77, no. 3-4, pgs. 361-370, March 2007.
- [58] Zhang, N.; and M. Kezunovic. *Transmission Line Boundary Protection Using Wavelet Transform and Neural Network*. IEEE Transactions on Power Delivery, vol. 22, no. 2, pgs. 859-869, April 2007.

- [59] Zhang, N.; and M. Kezunovic. *Verifying the Protection System Operation Using An Advanced Fault Analysis Tool Combined with the Event Tree Analysis*. Northern American Power Symposium, NAPS 2004 Moscow, Idaho, August 2004.
- [60] Vasilić, S.; and M. Kezunović. *Fuzzy ART Neural Network Algorithm for Classifying the Power System Faults*. IEEE Transactions on Power Delivery, vol. 20, no. 2, pgs. 1306-1314, April 2005.
- [61] Kezunović, M.; and I. Rikalo. *Detect and Classify Faults Using Neural Nets*. IEEE Computer Applications in Power, vol. 9, no. 4, pgs. 42-47, October 1996.
- [62] Diss.Zhang, Nan. *Advanced fault diagnosis techniques and their role in preventing cascading blackouts* Texas A&M University, 3246435, 2006.
- [63] Zhang, Nan; and M. Kezunovic. *A study of synchronized sampling based fault location algorithm performance during power swing*. St. Petersburg PowerTech' 05, St. Petersburg, Russia, June 2005.
- [64] Kezunovic, M.; B. Perunicic. *Automated Transmission Line Fault Analysis Using Synchronized Sampling at Two Ends*. IEEE Transactions on Power Systems, vol. 11, no. 1, pgs. 441-447, February 1996.
- [65] Kezunovic, M.; B. Perunicic, and J. Mrkic. *An Accurate Fault Location Algorithm Using Synchronized Sampling*. Electric Power Systems Research Journal, vol. 29, no. 3, pgs. 161-169, May 1994.
- [66] Keller, J.; M. R. Gray, and J. A. Givens. *A fuzzy K-nearest neighbor algorithm*. IEEE Transaction Systems, Man, Cybern., vol. SMC-15, no. 4, pgs. 580–585, July/August 1985.
- [67] Jacobs Sverdrup Incorporation System Safety and Risk Management Guide for Engineering Educators. Available at:
http://www.sverdrup.com/safety/riskmgt/lesson_9.pdf.
- [68] Gopalakrishnan, A.; M. Kezunovic, S.M. McKenna, and D.M. Hamai. *Fault Location Using Distributed Parameter Transmission Line Model*. IEEE Transactiona on Power Delivery vol. 15, no. 4, pgs. 1169-1174, October 2000.
- [69] Chang, Tim. *Impact of Distributed Generation on Distribution Feeder Protection*, University of Toronto (Canada), MR72537, 2010.
- [70] Lotfifard, S.; M. Kezunovic, and M.J. Mousavi. *Voltage Sag Data Utilization for Distribution Fault Location*. IEEE Transactions on Power Delivery vol. 26, no. 2, pgs. 1239-1246, April 2011.